AD_____

AWARD NUMBER: W81XWH-04-1-0824

TITLE: Molecular Mechanism of Nkx3.1 Deregulation and its Function in Murine Pten Prostate Cancer Model

PRINCIPAL INVESTIGATOR: Jing Jiao, Ph.D.

CONTRACTING ORGANIZATION: University of California
Los Angeles, California 90024

REPORT DATE: September 2006

TYPE OF REPORT: Annual Summary

PREPARED FOR: U.S. Army Medical Research and Materiel Command
Fort Detrick, Maryland 21702-5012

REPORT DOCUMENTATION PAGE

Form Approved
OMB No. 0704-0188

1. REPORT DATE *(DD-MM-YYYY)*	**2. REPORT TYPE**	**3. DATES COVERED** *(From - To)*
01-09-2006	Annual Summary	1 Sep 2004 – 31 Aug 2006

4. TITLE AND SUBTITLE

Molecular Mechanism of Nkx3.1 Deregulation and its Function in Murine Pten Prostate Cancer Model

5a. CONTRACT NUMBER

5b. GRANT NUMBER
W81XWH-04-1-0824

5c. PROGRAM ELEMENT NUMBER

6. AUTHOR(S)

Jing Jiao, Ph.D.

E-Mail: jjiao@mednet.ucla.edu

5d. PROJECT NUMBER

5e. TASK NUMBER

5f. WORK UNIT NUMBER

7. PERFORMING ORGANIZATION NAME(S) AND ADDRESS(ES)

University of California
Los Angeles, California 90024

8. PERFORMING ORGANIZATION REPORT NUMBER

9. SPONSORING / MONITORING AGENCY NAME(S) AND ADDRESS(ES)
U.S. Army Medical Research and Materiel Command
Fort Detrick, Maryland 21702-5012

10. SPONSOR/MONITOR'S ACRONYM(S)

11. SPONSOR/MONITOR'S REPORT NUMBER(S)

12. DISTRIBUTION / AVAILABILITY STATEMENT
Approved for Public Release; Distribution Unlimited

13. SUPPLEMENTARY NOTES

14. ABSTRACT

Both PTEN and Nkx3.1 play important role in prostate cancer control. Preliminary results from Pten prostate model indicated that reduced Nkx3.1 expression is correlated with Cre-mediated Pten deletion. The goal of this study is to investigate how these two proteins interplay in prostate cancer development.

We demonstrate that restoration of Nkx3.1 into Pten null prostate epithelium can lead to increases cell apoptosis, decreased cell proliferation and prevention of tumor initiation. The anti-tumor effect of Nkx3.1 is correlated with stabilization p53, inhibition Akt activation and AR function. This novel finding was published in Cancer cell. We generated and characterize the primary cell lines from Pten prostate cancer model, which will facilitate us to study the molecular mechanism of hormone refractory prostate cancer.

15. SUBJECT TERMS
No subject terms provided.

16. SECURITY CLASSIFICATION OF:			**17. LIMITATION OF ABSTRACT**	**18. NUMBER OF PAGES**	**19a. NAME OF RESPONSIBLE PERSON**
a. REPORT	**b. ABSTRACT**	**c. THIS PAGE**			USAMRMC
U	U	U	UU	54	**19b. TELEPHONE NUMBER** *(include area code)*

Standard Form 298 (Rev. 8-98)
Prescribed by ANSI Std. Z39.18

Table of Contents

INTRODUCTION

The *PTEN* tumor suppressor gene is one of the most frequently mutated/deleted genes in human prostate cancer, especially in advanced or metastatic forms[1]. Our murine *Pten* prostate cancer model mimics human prostate cancer development and provides an ideal experimental tool for characterization of the molecular events in disease initiation and progression[2]. Preliminary results from *Pten* prostate model indicated that reduced Nkx3.1 expression is correlated with Cre-mediated *Pten* deletion. Since loss of NKX3.1, which correlates with human prostate cancer initiation and progression, is regulated by unknown mechanism, the goal of this study is to investigate the mechanism by which PTEN regulate Nkx3.1 and to evaluate the role of Nkx3.1 loss in PTEN controlled prostate cancer development.

Two specific tasks should be accomplished in this study:

Task 1: To investigate the molecular mechanism by which PTEN regulates NKX3.1;
Task 2: To investigate the role of Nkx3. 1 loss in PTEN controlled prostate cancer development by tissue reconstitution assay.

BODY: STUDIES AND RESULTS

I. To investigate the molecular mechanism by which PTEN regulates NKX3.1

I-1. To establish and characterize epithelial cell lines corresponding to different stages of tumor development (finish)

To understand the molecular mechanisms underlying PTEN's dosage effects, we have generated two pairs of isogenic, androgen receptor (AR) positive prostate epithelial lines from hormone naïve *Pten* knockout mice that are either heterozygous (PTEN-P2 and –P8) or homozygous (PTEN-CaP2 and –CaP8) for *Pten* deletion. Despite no prior exposure to hormone ablation therapy, *Pten* null cells are tumorigenic on both male and female SCID mice, suggesting that PTEN intrinsically controls androgen responsiveness, a critical step in the development of hormone refractory prostate cancer. Although PTEN haploinsufficiency renders cells acquire androgen independence, heterozygous *Pten* deletion by itself is not sufficient for tumorigenesis. Furthermore, loss of the second allele of *Pten* leads to a higher level of androgen receptor expression, accelerated cell cycle progression and anchorage-independent growth without obvious structural or numerical chromosome changes based on the SKY karyotyping analysis. Importantly, knocking down AR by shRNA in *Pten* null cells completely reverse cell cycle phenotype in vitro and partially rescue tumorigenesis in vivo, indicating that PTEN controlled prostate tumorigenesis is AR-dependent. These cell lines will serve as useful tools for understanding signaling pathways controlled by PTEN and elucidating the molecular mechanisms involved in hormone refractory prostate cancer formation. (see attached manuscript)

I-2. To characterize Nkx3.1 expression, localization, and protein level in the established murine epithelial cells (partially finish)

Western analysis of primary cell lines generated from I-1 showed no Nkx3.1 protein expression. RT-PCR study from our murine Pten prostate cancer model showed that in 10 weeks, mutant prostate don't have Nkx3.1 transcription expression, which suggest that PTEN may regulate Nkx3.1 at the transcriptional level.

The dosage effect of PTEN regulation on Nkx3.1 expression will be examined in heterozoyte *Pten* prostate tissue.

I-3. To study the molecular mechanism controlling NKX3.1 degradation (partially finish)

Ongoing study for task 1 part is to continue exam the role of PTEN in regulating Nkx3.1 transcription and protein stability: 1) I will generate lucififase-Nkx3.1 promoter and exam PTEN'S role in transcriptional regulation. To increase the transcription efficiency, I will use the inducible Pten lenti-construct; 2) I will use the cell line generate in this study as well as human cell lines to exam the role of PTEN on Nkx3.1 post-transcriptional expression.

II. To investigate the role of Nkx3.1 loss in PTEN controlled prostate cancer development

II-1. Reintroduce Nkx3.1 into *Pten* null prostate epithelium and test its effect on prostate cancer development **(Accomplished, for detail, see attached publication)**

Using renal capsule prostate reconstitution assay[3] with the collaboration with another postdoc(Lei qunyin) in our lab, we demonstrated that restoration of *Nkx3.1* expression to the WT level in the *Pten* null epithelium leads to decreased cell proliferation, increased cell death and prevention of tumor initiation.

Significantly, by reintroducing Nkx3.1 into the Pten-CaP2 cells, we observed the increased p53 expression and decreased AR expression. The positive regulation of p53 by Nkx3.1 was further confirmed in human Lncap cell line as well as Nkx3.1 knock out prostate tissue. RT-PCR analysis and p53 half-life study demonstrated that Nkx3.1 regulated p53 at the post-transcriptional level. I further demonstrated that NKX3.1 stabilizes p53 through MDM2-dependent and AKT-independent mechanisms, regulates androgen receptor (AR) transcription and inhibits AKT activation in AR-dependent manner.

Wwe further demonstrated that NKX3.1 engages cell cycle and cell death machinery via association with HDAC1, leading to increased p53 acetylation and half-life through MDM2-dependent mechanisms.

II-2. Test the molecular mechanism by which Pten modulates Nkx3.1 in the tissue reconstitution assay

Since we can successfully reintroduce *Nkx3.1* expression using an exogenous promoter, and maintain near WT levels of NKX3.1 in different PTEN null cell lines and in the renal capsule grafts, it suggest that PTEN may modulate NKX3.1 expression largely through regulation of its transcription. Therefore, it also gave us the new focus in Aim I-3.

KEY RESEARCH ACCOMPLISHMENTS

- Establish and characterize of primary cell lines from Pten-null prostate tissue and provide insight on the role of PTEN on HRPC

- Finish the investigation of Nkx3.1's role in PTEN controlled cancer initiation and progression (task 2) and published the data on Cancer Cell

REPORTABLE OUTCOMES

- Publication

  Qunying Lei, **Jing Jiao**, Li Xin, Chun-Ju Chang, Shunyou Wang, Jing Gao, Martin E. Gleave, Owen N. Witte, Xin Liu, and Hong Wu (2006) NKX3.1 stabilizes p53, inhibits AKT activation, and blocks prostate cancer initiation caused by PTEN loss *Cancer Cell.* 2006 May;9(5):367-78.

  Jing Jiao, Qunyin Lei, Shunyou Wang, Hong Wu (2003) Establishment and characterization of primary epithelial cell lines from Murine *Pten* prostate cancer model. In: Ninty-six Annual Meeting of the American Association for Cancer Research, Anaham, April 2005

CONCLUSIONS

During the second funding period of this project, we have accomplished the task 2 and get the paper published in *Cancer Cell*. Based on our study, we proposed a model: in *Pten* wild-type prostatic epithelium, PTEN negatively regulates PI3K/AKT pathway but positively modulates p53 level and activity. The transcription level of Nkx3.1 is controlled predominantly by PTEN as well as by AR. NKX3.1 in turn negatively regulates AR promoter activity and keeps AR and AR-controlled pathway in check. NKX3.1 also binds HDAC1 and releases p53 from p53-MDM2-HDAC1 complex, promoting p53 acetylation and activity. The net result of these NKX3.1-mediated PTEN functions is the balanced cell proliferation, differentiation, and cell death, which prevents prostate cancer initiation. Upon PTEN loss, the balance is broken, and NKX3.1 and its controlled signaling pathways are severely downregulated. AR, no longer under the control of NKX3.1, becomes overexpressed and activates its targets and downstream pathways, including PI3K/AKT pathway. In the absence of NKX3.1, most of the p53 is in the MDM2-HDAC1 complex, leading to p53 degradation. Activation of PI3K/AKT pathway, together with downregulated p53 activity and increased AR level and activity, leads to increased cell proliferation, decreased cell death, and prostate cancer initiation [4]. This part of study highlights the important role of Nkx3.1 in preventing tumor

initiation and the collaboration of the two tumor suppressor in prostate disease control.

We generated the primary epithelial cells from Pten null prostate for task 1. We further PTEN controlled prostate tumorigenesis is AR-dependent. These cell lines will serve as useful tools for understanding signaling pathways controlled by PTEN and elucidating the molecular mechanisms involved in hormone refractory prostate cancer formation.

REFERENCES

1. Porkka, K.P. and T. Visakorpi, *Molecular mechanisms of prostate cancer.* Eur Urol, 2004. **45**(6): p. 683-91.
2. Wang, S., et al., *Prostate-specific deletion of the murine Pten tumor suppressor gene leads to metastatic prostate cancer.* Cancer Cell, 2003. **4**(3): p. 209-21.
3. Xin, L., et al., *In vivo regeneration of murine prostate from dissociated cell populations of postnatal epithelia and urogenital sinus mesenchyme.* Proc Natl Acad Sci U S A, 2003. **100 Suppl 1**: p. 11896-903.
4. Lei, Q., et al., *NKX3.1 stabilizes p53, inhibits AKT activation, and blocks prostate cancer initiation caused by PTEN loss.* Cancer Cell, 2006. **9**(5): p. 367-78.

APPENDICES

- Publication

  Qunying Lei, **Jing Jiao**, Li Xin, Chun-Ju Chang, Shunyou Wang, Jing Gao, Martin E. Gleave, Owen N. Witte, Xin Liu, and Hong Wu (2006) **NKX3.1 stabilizes p53, inhibits AKT activation, and blocks prostate cancer initiation caused by PTEN loss *Cancer Cell.* 2006 May;9(5):367-78.**

  Manuscript

  Jing jiao, Shunyou Wwang, Rong qiao, Igor Vivanco, Philip A. Watson, Charles L. Sawyers, Hong Wu **Novel Murine Prostate Cancer Cell Lines Provide Insight into PTEN's Dosage Effect on tumorigenesis and Androgen Responsiveness (in preparation)**

NKX3.1 stabilizes p53, inhibits AKT activation, and blocks prostate cancer initiation caused by PTEN loss

Qunying Lei,[1] Jing Jiao,[1] Li Xin,[2] Chun-Ju Chang,[1] Shunyou Wang,[1] Jing Gao,[1] Martin E. Gleave,[5] Owen N. Witte,[1,2,3] Xin Liu,[1,4] and Hong Wu[1,*]

[1] Department of Molecular and Medical Pharmacology, David Geffen School of Medicine at the University of California, Los Angeles, Los Angeles, California 90095
[2] Department of Microbiology, Immunology, and Molecular Genetics, David Geffen School of Medicine at the University of California, Los Angeles, Los Angeles, California 90095
[3] Howard Hughes Medical Institute, David Geffen School of Medicine at the University of California, Los Angeles, Los Angeles, California 90095
[4] Department of Pathology and Laboratory Medicine, David Geffen School of Medicine at the University of California, Los Angeles, Los Angeles, California 90095
[5] The Prostate Centre at Vancouver General Hospital, Vancouver, British Columbia V6H 3Z6, Canada
*Correspondence: hwu@mednet.ucla.edu

Summary

We demonstrate that PTEN loss causes reduced NKX3.1 expression in both murine and human prostate cancers. Restoration of *Nkx3.1* expression in vivo in *Pten* null epithelium leads to decreased cell proliferation, increased cell death, and prevention of tumor initiation. Whereas androgen receptor (AR) positively regulates NKX3.1 expression, NKX3.1 negatively modulates AR transcription and consequently the AR-associated signaling events. Consistent with its tumor suppressor functions, NKX3.1 engages cell cycle and cell death machinery via association with HDAC1, leading to increased p53 acetylation and half-life through MDM2-dependent mechanisms. Importantly, overexpression of *Nkx3.1* has little effect on *Pten* wild-type epithelium, suggesting that PTEN plays a predominant role in PTEN-NKX3.1 interplay. Manipulating NKX3.1 expression may serve as a therapeutic strategy for treating PTEN-deficient prostate cancers.

Introduction

Prostate cancer is the second leading cause of cancer-related death in males (Gregorakis et al., 1998; McDavid et al., 2004). Its development proceeds through a series of defined steps, including prostatic intraepithelial neoplasia (PIN), invasive cancer, and hormone-dependent or -independent metastasis. Although different stages of prostate cancer have been well defined histologically, relatively little is known about the molecular mechanisms contributing to the initiation and progression of prostate cancer.

The *PTEN* (phosphatase and tensin homolog deleted on chromosome 10) tumor suppressor gene is frequently mutated in human cancers (Dahia, 2000; Maehama et al., 2001; Parson et al., 1998). The major function of PTEN relies on its phosphatase activity toward PIP3 (phosphatidyl inositol 3,4,5-triphosphate) and, consequently, antagonism of the PI3K (phosphatidylinositol 3-kinase) signaling pathway (Di Cristofano et al., 2001; Maehama et al., 2001). Loss of *PTEN* function results in accumulation of PIP3 and activation of its downstream effectors, such as AKT/PKB (Maehama et al., 2001). AKT, a serine/threonine protein kinase, phosphorylates key intermediate signaling molecules, leading to increased cell metabolism, growth, survival, and invasiveness, all hallmarks of cancer (Di Cristofano et al., 2001; Hanahan and Weinberg, 2000; Vivanco and Sawyers, 2002).

PTEN alteration is strongly implicated in prostate cancer development, as mutations of the *PTEN* gene are found in 30% of primary prostate cancers (Dahia, 2000; Sellers and Sawyers, 2002) and 63% of metastatic prostate tissue samples (Suzuki et al., 1998). Thus, *PTEN* mutations are among the most frequent genetic alterations in human prostate cancer. As PTEN-controlled signaling pathways are frequently altered in human prostate cancers, inhibiting the resultant signaling aberrations will likely serve as promising targets for therapeutic strategies

SIGNIFICANCE

Gene expression profiling of mouse tumor models or human cancers has identified many dysregulated genes that may contribute to tumor development. These wealthy data sets, upon functional validation, may help in elucidating the molecular mechanisms underlying tumorigenesis and providing potential novel targets for cancer therapies. Using a powerful prostate epithelial tissue reconstitution assay, we demonstrated the importance of NKX3.1 in prostate cancer initiation caused by PTEN loss. Our finding emphasizes the cooperative effects between ubiquitously expressed *PTEN* tumor suppressor genes and prostate-specific expressed *NKX3.1* in prostate cancer development. Our study further indicates that validation of candidate genes using mouse models can yield valuable molecular insights that impact human cancer research.

(DeMarzo et al., 2003; Sellers and Sawyers, 2002; Vivanco and Sawyers, 2002).

We and others have developed murine models of prostate cancers by deleting the *Pten* tumor suppressor gene specifically in the prostatic epithelium (Chen et al., 2005; Ma et al., 2005; Trotman et al., 2003; Wang et al., 2003). The *Pten* prostate cancer model recapitulates many features of the disease progression seen in humans with defined kinetics: initiation of prostate cancer with PIN lesions, followed by progression to locally invasive adenocarcinoma, and subsequent metastasis (Wang et al., 2003). Similar to human cancer, *Pten* null murine prostate cancers regress in response to androgen ablation therapy but subsequently relapse and proliferate in the absence of androgens (Wang et al., 2003).

Global assessment of molecular changes caused by homozygous *Pten* deletion identified key genes known to be relevant to human prostate cancer, including those "signature" genes associated with human cancer metastasis (Wang et al., 2003). Among the genes that are downregulated in *Pten* null prostate cancer is *Nkx3.1*, a homeobox gene specifically expressed in the prostate epithelium. NKX3.1 is one of the earliest markers for prostate development and is continuously expressed at all stages during prostate development and in adulthood (Bhatia-Gaur et al., 1999). Human *NKX3.1* maps to chromosome 8p21, a region that frequently undergoes loss of heterozygosity (LOH) at early stages of prostate carcinogenesis (He et al., 1997; Voeller et al., 1997). *Nkx3.1* mutant mice develop prostatic hyperplasia and dysplasia. However, these early lesions failed to progress to metastatic cancers (Abdulkadir et al., 2002; Bhatia-Gaur et al., 1999), consistent with a role for *Nkx3.1* inactivation in prostate cancer initiation.

In this study, we employed a dissociated prostatic epithelial regeneration system to directly test the significance of *Nkx3.1* loss in *Pten* null prostate cancer formation. Our data show that NKX3.1 plays an important role in prostate cancer initiation caused by PTEN loss and that forced *Nkx3.1* expression prevents *Pten* null prostate cancer initiation and progression. Thus, decreased *Nkx3.1* expression contributes to prostate cancer development caused by PTEN loss.

Results

PTEN loss leads to reduced *NKX3.1* expression in both murine and human prostate cancers

Our previous gene expression profiling analysis revealed that *Nkx3.1* mRNA level is downregulated in the *Pten* null prostate cancers (Wang et al., 2003). In this study, consecutive sections of ventral prostate lobe from 4-week-old (4W) *Pten* conditional knockout animals were probed with antibodies to either NKX3.1 or phospho-AKT (P-AKT/Ser 473) (Figure 1A). In the acini where P-AKT levels are low, intense NKX3.1 staining can be observed (Figure 1A, arrows). In contrast, areas with high P-AKT are either low or negative for NKX3.1 staining (Figure 1A, arrowheads). Since increased AKT phosphorylation is a consequence of PTEN loss (Figure S1 in the Supplemental Data available with this article online), these staining patterns suggest that *Nkx3.1* downregulation is an early event linked to *Pten* deletion and prostate cancer initiation.

To test whether PTEN-regulated *Nkx3.1* expression can be observed in human prostate cancers, we conducted double immunofluorescent analysis of PTEN and NKX3.1, using human

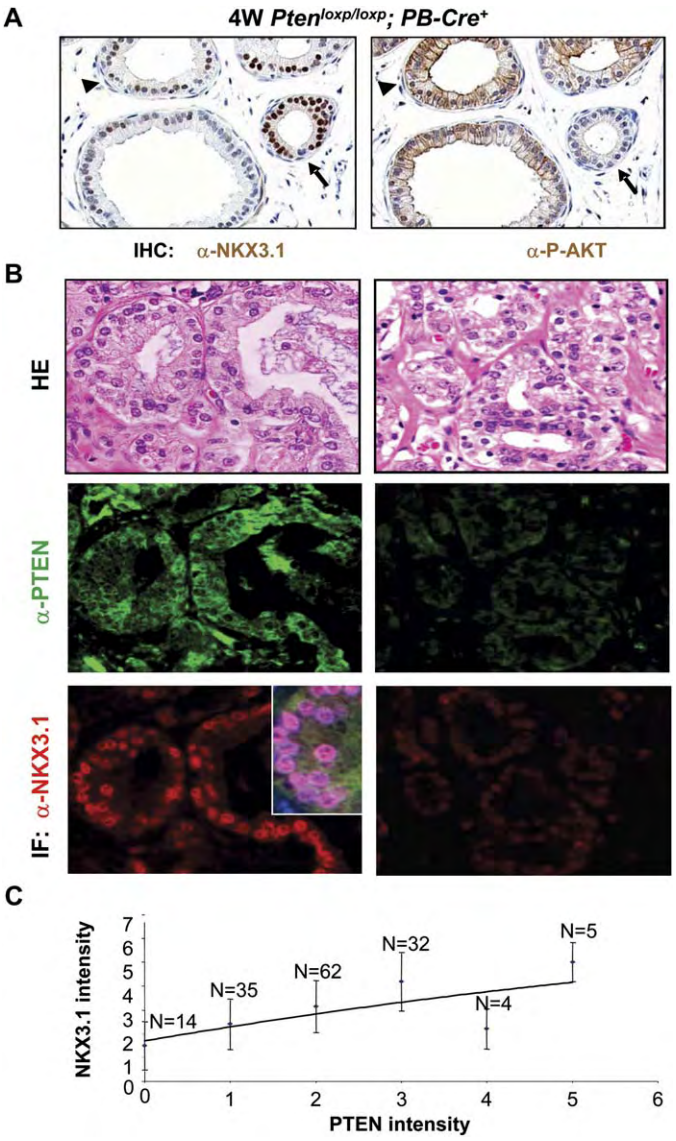

Figure 1. PTEN loss leads to decreased NKX3.1 protein levels in both murine and human prostate epithelium

A: Consecutive sections of 4-week-old *Pten* mutant prostates were probed for NKX3.1 (left) and phospho-AKT (Ser 473) (P-AKT, right) expression. Arrows and arrowheads point to the same duct. Note that NKX3.1 expression reversely correlates with P-AKT staining.

B: High-magnification views of two representative samples from human prostate cancer tissue microarray are shown here. Upper panels: H&E staining; middle and lower panels: double immunofluorescent staining using anti-PTEN (middle) and anti-NKX3.1 (lower) antibodies. Insert: high-power overlay of NKX3.1 and DAPI staining showing NKX3.1 nuclear localization.

C: Correlation of PTEN and NKX3.1 protein levels in 153 human prostate samples. SPSS liner regression was used to analyze data, and the standardized coefficient value was 0.52 ($p < 0.01$ level; $n = 153$).

prostate tissue microarrays (Rocchi et al., 2004). Among 153 samples surveyed (see Experimental Procedures), positive PTEN expression was significantly correlated with NKX3.1 staining, whereas PTEN loss was associated with decreased NKX3.1 staining (Figure 1C; $p < 0.01$). Photos from two representative samples are shown in Figure 1B. Therefore, PTEN loss leads to decreased NKX3.1 expression in both human and murine prostate cancers, implying that NKX3.1 may serve

as an important regulator downstream of PTEN-controlled signaling pathway in prostate cancer development.

Forced *Nkx3.1* expression in *Pten* null epithelium using an exogenous promoter

Several mechanisms have been proposed for loss of NKX3.1 expression in human prostate cancers, including both transcriptional and posttranscriptional regulations (Asatiani et al., 2005; Bowen et al., 2000; He et al., 1997; Korkmaz et al., 2004; Ornstein et al., 2001; Voeller et al., 1997). To understand how PTEN controls NKX3.1 expression and to evaluate the functional relevance of *Nkx3.1* downregulation in *Pten* null prostate cancer initiation, we employed a dissociated prostate cell regeneration method (Xin et al., 2003, 2005) to test (1) whether we can restore NKX3.1 expression in *Pten* null epithelium to a level comparable to the wild-type (wild-type) by using an exogenous promoter, and (2) the consequence of forced *Nkx3.1* expression in *Pten* null prostate epithelium. In order to circumvent the low transfection efficiency of mouse prostate epithelium, we cloned Flag-tagged *Nkx3.1* into a lentiviral vector (Xin et al., 2003, 2005) in which *Nkx3.1* expression is driven by the ubiquitin promoter followed by an IRES-eGFP expression cassette (Figure 2A) (Lois et al., 2002). NKX3.1 expression can be detected indirectly via eGFP expression (Figure 2B, left panels) and by Western blot analysis of transfected 293T cells using total protein lysate (Figure 2B, upper row in the right panel) or eGFP-sorted cells (Figure 2B, middle row in the right panel) with an anti-Flag antibody.

We then infected epithelium from 4W *Pten* null mice (Mut), corresponding to the hyperplastic stage, and the epithelium from their wild-type littermates with *Nkx3.1* expressing (NKX3.1 group) or control lentivirus (GFP group). Infected epithelium was then mixed with mesenchyme isolated from embryonic day 16 wild-type urogenital sinus mesenchyme (UGSM) and grafted under the renal capsule of $CB17^{SCID/SCID}$ mice and propagated for 6 weeks. Low but detectable levels of PTEN expression can be found in the mutant grafts by Western blot analysis (Figure 2C, insert), most likely attributable to the wild-type UGSM cells used for reconstitution. Importantly, lentivirus-mediated gene expression in *Pten* null grafts restored NKX3.1 protein levels so that they were comparable to those of the WT graft (Figure 2C, insert). The fact that NKX3.1 protein expression can be restored and maintained near the wild-type levels via an exogenous promoter suggests that PTEN modulates NKX3.1 function largely through regulation of its transcription, e.g., by controlling its promoter activity.

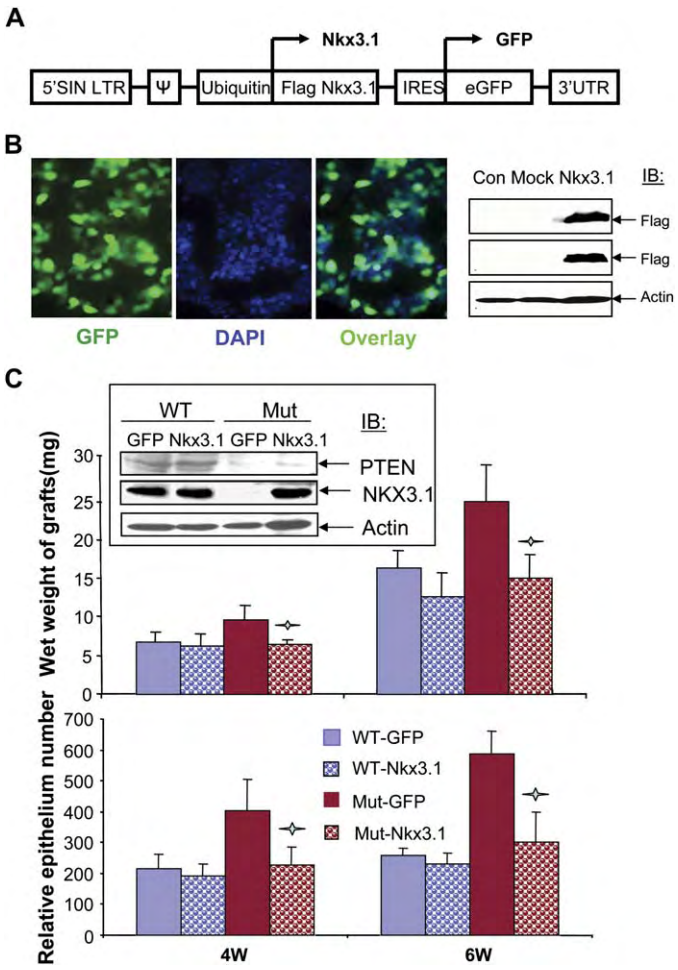

Figure 2. Overexpression of *Nkx3.1* reduces the growth of reconstituted *Pten* null epithelium graft

A: The lentivirus FUGW-IRES-eGFP vector used for expressing *Nkx3.1*.

B: NKX3.1 expression can be indirectly detected by the expression of GFP from the same vector (left panels). Right panels show the expression of Flag-tagged NKX3.1 protein in 293T cells (upper row) and infected, eGFP-sorted cells (middle row) by Western blot analysis.

C: A comparison of the wet weight (upper panel) and relative epithelial cell number (lower panel) of regenerated tissue without or with forced *Nkx3.1* expression (mean ± SD). Similar results were obtained in three independent experiments ($p \leq 0.05$). Insert: Western blot shows the levels of PTEN and NKX3.1 in mock-infected (GFP group) and NKX3.1 viral-infected (Nkx3.1 group) grafts.

Introducing *Nkx3.1* into *Pten* null prostatic epithelium leads to reduced graft growth

To evaluate the effects of PTEN loss and forced NKX3.1 expression, we quantified the graft weight (Figure 2C, upper panel) and DNA contents (Figure S2). To increase the confidence of our analysis, we considered only the epithelial compartment, instead of both the mesenchymal and epithelial ones, as a function of PTEN loss or forced *Nkx3.1* expression (Figure 2C, lower panel). Compared to wild-type grafts (blue), *Pten* null grafts (in red) are significantly larger and include greater number of epithelium (Figure 2C, left, compare wild-type-GFP and Mut-GFP groups) while forced *Nkx3.1* expression consistently reduced *Pten* null graft weight and epithelial cell numbers (Figure 2C, compare Mut-GFP and Mut-Nkx3.1 grafts; $p < 0.05$). To evaluate whether the effect of forced *Nkx3.1* expression depends on the stage of cancer, epithelium from PIN lesions (6W) were harvested and yielded similar observations (Figure 2C, right). No significant difference was observed when mock-infected wild-type grafts were compared to *Nkx3.1*-infected wild-type grafts (Figure 2C, compare wild-type-GFP and wild-type-Nkx3.1 groups). These data show that forced *Nkx.3.1* expression can reverse the growth advantage of *Pten* null epithelium but has little effects on its wild-type counterpart.

Nkx3.1 blocks *Pten* null prostate cancer initiation and progression

Histological analysis indicated that wild-type and *Pten* null epithelium reconstituted prostate grafts recapitulate the

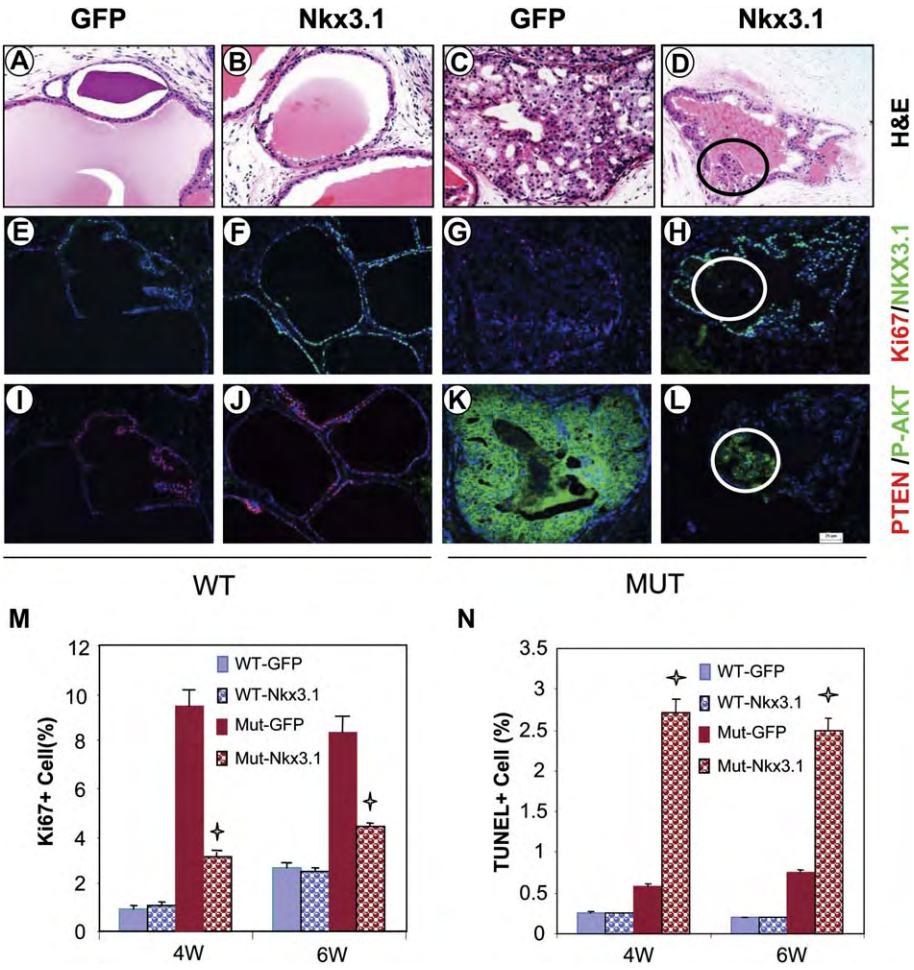

Figure 3. *Nkx3.1* reexpression in *Pten* null epithelium leads to decreased cell proliferation, increased cell death, and reverse of hyperplasia phenotype

A–D: Histopathology of regenerated grafts. H&E-stained paraffin sections of grafts generated from 4-week-old wild-type (**A** and **B**) and *Pten* null (MUT) epithelium (**C** and **D**). Circled area in **D** appears hyperplastic in otherwise normal duct.

E–L: Consecutive sections from upper panels were double immunofluorescent stained with anti-Ki67 and -NKX3.1 antibodies (**E**–**H**), as well as anti-PTEN and -P-AKT antibodies (**I**–**L**) and then counterstained with DAPI. Circled area shows negative correlation of P-AKT staining (**L**) with NKX3.1 expression (**H**).

M and N: *Nkx3.1* reexpression in *Pten* null epithelium leads to quantitatively decreased cell proliferation (M) and increased cell death (N). Data are represented as mean ± SD from three independent experiments ($p \leq 0.05$).

histological characterization of the donor epithelium (Figures 3A and 3C)(Wang et al., 2003). No significant difference was observed when comparing wild-type-GFP and wild-type-Nkx3.1 grafts (compare Figures 3A and 3B). In contrast, tissue recombinants from *Pten* null epithelium resulted in very differential phenotypes: those from the GFP group demonstrated hyperplasia and early mPIN lesions, whereas grafts from the *Nkx3.1* expression group showed relative preservation of normal prostatic duct structure with protein secretion in the lumen (compare Figures 3C and 3D). Occasionally, isolated areas with hyperplastic phenotype were observed (Figure 3D, circled area). Further studies using consecutive sections suggest that these hyperplastic lesions are most likely due to incomplete viral infection, as evidenced by the low to undetectable NKX3.1 protein expression and high P-AKT staining in the same region (circled areas in Figures 3H and 3L, respectively). These results suggest that forced *Nkx3.1* expression can rescue the hyperplastic phenotype caused by PTEN loss.

Forced *Nkx3.1* expression leads to decreased cell proliferation and increased apoptosis of *Pten* null grafts

Previous studies showed that overexpression of *NKX3.1* in human PC3 prostate cancer cells and rodent AT 6 cells leads to inhibition of cell growth (Kim et al., 2002a), whereas increased epithelial cell proliferation is observed in *Nkx3.1* knockout mice (Abdulkadir et al., 2002; Bhatia-Gaur et al., 1999; Magee et al., 2003; Tanaka et al., 2000). We examined whether forced *Nkx3.1* expression could inhibit cell proliferation in *Pten* null epithelium grafts. Detection of the Ki-67 epitope indicated that *Nkx3.1* expression significantly decreased the proliferative index of 4W and 6W mutant grafts (compare Figures 3G and 3H; quantification shown in Figure 3M; $p \leq 0.05$) consistent with the growth-suppressive function of NKX3.1 in previous studies. Interestingly, *Pten* null epithelium appears to be hypersensitive to NKX3.1's suppression effect, since NKX3.1 at similar protein levels (Figure 2C, insert) has no significant effect on cell proliferation in the wild-type grafts (Figures 3E, 3F, and 3M).

Given that *Pten* null grafts infected with NKX3.1 were consistently smaller than those of the control GFP group (Figure 2C), the apoptotic index was evaluated by way of the TUNEL assay. In both 4W and 6W *Pten* null grafts, a significant increase in TUNEL-positive cells was observed in the presence of NKX3.1 (Figure 3N; $p \leq 0.05$). When consecutive tissue sections were probed for the presence of NKX3.1, TUNEL-positive cells were consistently associated with areas of strong NKX3.1 expression (Figure S3). No increase in TUNEL-positive cells was observed in 4W or 6W wild-type grafts (Figure 3N). Taken together, our data demonstrate that the effects of NKX3.1 on cell proliferation and cell death depend on the PTEN status.

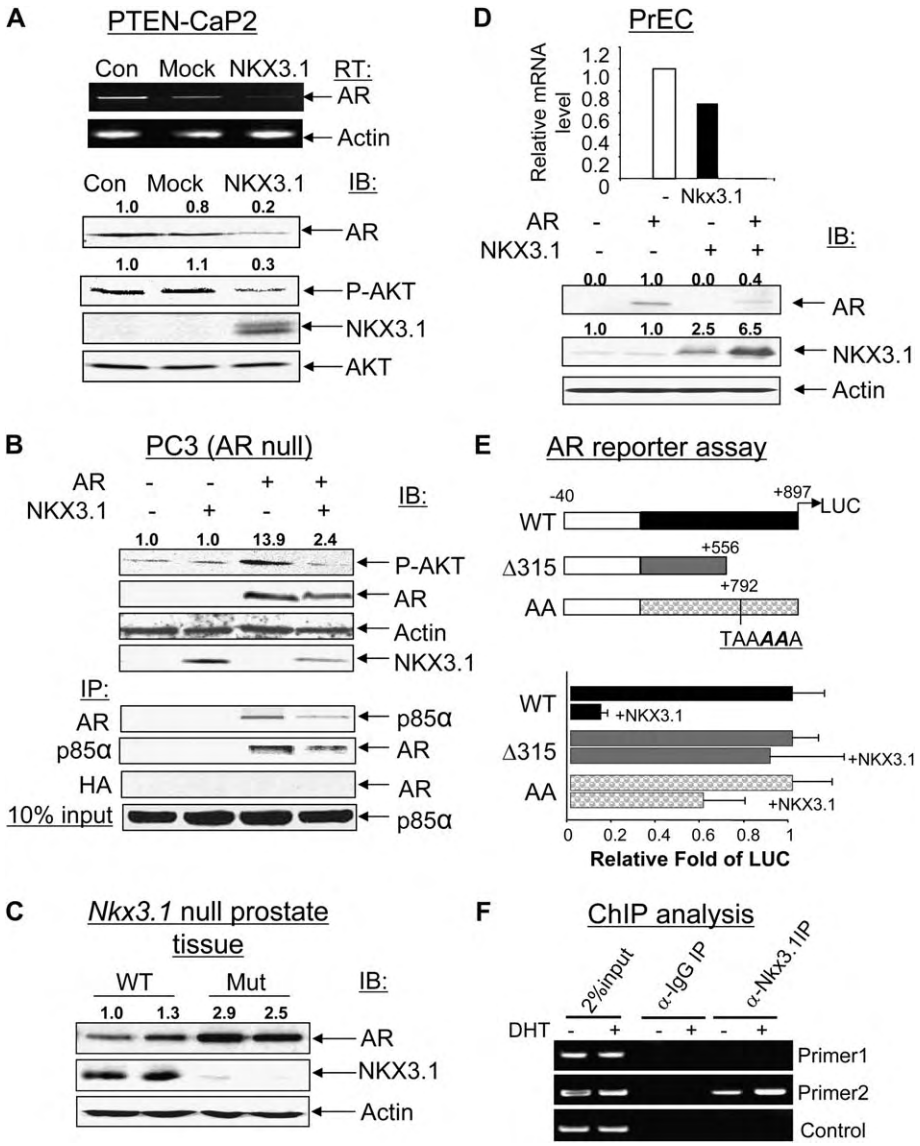

Figure 4. NKX3.1 negatively regulates AR promoter and modulates AKT phosphorylation through an AR-dependent mechanism

A: NKX3.1 regulates AR transcription and reduces AKT phosphorylation in vitro. Total RNA and protein were harvested from PTEN-CaP2 cells transfected with *Nkx3.1*. RT-PCR (upper panel), and Western blot analysis (lower panel) was performed as indicated.

B: NKX3.1-regulated AKT phosphorylation depends on AR expression. PC3 cells were transfected with *Nkx3.1* without *AR* (left two lanes) and with *AR* (right two lanes). Cell lysates were immunoprecipitated with indicated antibodies and analyzed by Western blotting. P-AKT levels were normalized to actin levels.

C: Loss of NKX3.1 leads to increased AR expression in vivo. Western blot analysis of wild-type and *Nkx3.1* null prostate tissues. AR expression levels were normalized to actin loading control.

D: NKX3.1 regulates AR expression in normal human primary prostatic cells. PrEC cells were transfected with indicated plasmid. Thirty-six hours later, RNA and protein were harvested for real-time PCR (upper panel) and Western blot analysis (lower panel), respectively. AR expression and NKX3.1 expression levels were normalized to actin levels.

E: NKX3.1 suppresses AR transcription. PTEN-CaP2 cells were cotransfected with AR luciferase reporter constructs and NKX3.1 expression vector. Relative AR transcriptional activity was measured 24 hr posttransfection. Three independent tests were performed for each experiment and presented as mean ± SD.

F: Association of endogenous NKX3.1 with the AR promoter. LNCaP cells were treated with or without DHT (10 nM) for 16 hr, and ChIP analysis was performed according to Experimental Procedures.

NKX3.1 negatively regulates AKT activity in an AR-dependent manner

To investigate possible changes in the known PTEN-controlled signaling pathways in the presence and absence of NKX3.1, we first examined AKT status on consecutive sections of the grafts. No difference in either PTEN or P-AKT levels can be detected in the wild-type grafts with or without *Nkx3.1* overexpression (Figures 3I and 3J). Robust P-AKT staining can be detected in the mock-infected *Pten* null grafts (Figure 3K), whereas forced *Nkx3.1* expression, at a level comparable to that of wild-type prostatic epithelium (compare Figures 3F and 3H, and Figure 2C), leads to a dramatic decrease in P-AKT levels (Figure 3L). In the uninfected area where NKX3.1 staining is weak or undetectable (Figure 3H, circled area), P-AKT level remains high, thus serving as an important internal control (Figure 3L, circled area).

To develop a system more amenable to in vitro biochemical analysis, we generated several prostate epithelial cell lines from the prostates of *Pten* conditional knockout mice. One such line, PTEN-CaP2, is characterized by positive AR expression but undetectable PTEN and NKX3.1 protein expression (our unpublished data). *Nkx3.1* overexpression in PTEN-CaP2 cells suppressed AKT phosphorylation by 3-fold (Figure 4A, lower panel).

Given previous studies that androgen receptor (AR) can modulate AKT activation via a PI3K-dependent mechanism (Baron et al., 2004; Sun et al., 2003), we investigated whether AR serves as a mediator for NKX3.1-regulated AKT activity. For this, we used PC3 cells, a human prostate cancer cell line known to be null for AR, PTEN, and NKX3.1. When we compared P-AKT levels in the presence or absence of NKX3.1 without cotransfection of AR, we did not detect any significant difference (Figure 4B, first two lanes in the upper panel). While introduction of AR significantly increased the level of P-AKT (Figure 4B, compare first and third lanes in the upper panel), this effect was diminished by cotransfection of the *Nkx3.1*-expressing vector (Figure 4B, compare the third and fourth lanes). Previous studies also showed that AR modulates AKT phosphorylation via binding of the p85α subunit of PI3-kinase (Baron et al., 2004; Sun et al., 2003). We performed reciprocal coimmunoprecipitation experiments and showed that *Nkx3.1* overexpression decreases the

amount of AR able to interact with p85α (Figure 4B, lower panels), further supporting the notion that NKX3.1 controls AKT phosphorylation via an AR/PI3K-dependent mechanism.

NKX3.1 negatively regulates the AR promoter

Since AR serves as a mediator for NKX3.1-controlled AKT activation, we investigated the possible role of NKX3.1 on AR expression in the PTEN-CaP2 cells and found that NKX3.1 also inhibits AR expression at both mRNA (Figure 4A, upper panel) and protein levels (Figure 4A, lower panel). To determine if NKX3.1 negatively regulates AR in vivo, we examined AR protein levels in the prostate glands of *Nkx3.1* knockout mice (Kim et al., 2002b) and found that AR levels are indeed increased (Figure 4C). The role of NKX3.1 in negatively regulating AR level was also confirmed in human primary prostatic PrEC cells (Figure 4D, upper panel; compare lanes 2 and 4 in the lower panel).

Similar to previous reports (Bieberich et al., 1996; He et al., 1997; Magee et al., 2003; Prescott et al., 1998), our study indicates that NKX3.1 expression can be positively modulated by androgen (Figure 4D, compare lanes 3 and 4; Figure 6B). That overexpression of NKX3.1 leads to AR downregulation (upper panels in Figures 4A and 4D) while NKX3.1 loss results in an increased level of AR (Figure 4C) suggests that AR and NKX3.1 may form an important feedback loop. Within this feedback loop, NKX3.1 may serve as an important negative regulator for AR expression as well as AR-controlled signaling pathway. To test this hypothesis, we searched sequences surrounding the murine AR promoter region and found a potential NKX3.1 consensus binding site, TAAGTA, within the 5′ UTR. The functional significant of this consensus site was further investigated using a series of luciferase reporter constructs with truncated promoter regions (Figure 4E, upper panel). NKX3.1 significantly suppressed the wild-type reporter construct, while it had little effect on a Δ315 construct in which sequences surrounding the putative binding motif have been deleted (Figure 4E, lower panel). Changing ''TAAGTA'' to ''TAAAAA'' also decreased NKX3.1's effect (Figure 4E, lower panel).

To assess whether NKX3.1 can associate with the endogenous AR promoter, we conducted chromosome immunoprecipitate (ChIP) analysis on the human prostate cancer cell line LNCaP, which expresses endogenous NKX3.1 and AR. Using a primer set that contains the human NKX3.1 ''CAAG'' motif (nt 1223–1386), we showed that the endogenous NKX3.1 can physically associate with the AR promoter and that this association can be further enhanced in the presence of androgen (Figure 4F, primer 2). We further demonstrate that this association is site specific: primer 1 set derived from nt 1113–1311 of the human AR promoter containing the ''CAAG'' motif, as well as control primers (nt 17–170) without the CAAG motif, can not detect NKX3.1 binding activity. Therefore, NKX3.1 inhibits AR transcriptional activity, at least in part, through its consensus binding site.

NKX3.1 negatively regulates AR expression in both murine and human prostatic cancer samples

To test whether the inverse relationship between NKX3.1 and AR is present in human prostate cancer samples, we conducted double immunofluorescent analysis of NKX3.1 and AR and found two basic scenarios: areas where NKX3.1 levels negatively correlate with AR levels (Figure 5A) and areas where NKX3.1 and AR are coexpressed (Figure 5B). Interestingly, even in the areas where both NKX3.1 and AR are expressed, mosaic patterns of NKX3.1 and AR expression can be easily detected (Figure 5B, high-powered image on the right), suggesting that the NKX3.1-AR feedback loop may function at a single cell level.

Importantly, despite upregulated AR levels (Figure 5C), NKX3.1 mRNA levels are downregulated in both PIN (Figure 5C) and *Pten* null prostate cancer (Wang et al., 2003), suggesting that PTEN either plays a predominant role over AR, the known positive regulator of *Nkx3.1*, or is essential for AR-mediated *Nkx3.1* regulation. We then compared the relative expression levels of those NKX3.1 target genes identified by Magee et al. (2003) that are also present in our microarray data sets (Wang et al., 2003 and our unpublished data). Intriguingly, the trends of gene regulation in the *Pten* null prostate are very similar to what has been observed in the *Nkx3.1* null prostate: *Probasin*, which is known to be positively regulated by NKX3.1, is downregulated in the *Pten* null PIN lesions, whereas *Elafin-like II*, which belongs to the repression group, is upregulated upon *Pten* deletion (Figure 5C). Furthermore, the mosaic expression patterns of NKX3.1 and AR shown in Figure 5B may provide an explanation for the stochastic expression patterns of NKX3.1-targeted genes within the same prostatic acini (Magee et al., 2003).

NKX3.1 stabilizes p53 through MDM2-dependent and AKT-independent mechanisms

PTEN regulates p53 protein levels and transcription activity via AKT-MDM2-dependent and -independent mechanisms (Freeman et al., 2003; Mayo and Donner, 2001; Zhou et al., 2001). The fact that overexpression of NKX3.1 inhibits AKT phosphorylation in *Pten* null grafts prompts us to analyze whether NKX3.1 also alters p53 levels. Western blot analysis demonstrated that forced *Nkx3.1* expression significantly increases p53 protein levels in *Pten* null grafts in vivo (Figure 6A, upper panels), whereas knockout of *Nkx3.1* leads to reduced p53 levels (Figure 6A, lower panels).

To understand the molecular mechanisms involved in NKX3.1-regulated p53 activity, we first measured endogenous p53 levels in the LNCaP cells. The androgen analog R1881 can stimulate the endogenous NKX3.1 expression with a peak around 4 hr (Figure 6B, upper panel). Following this trend, p53 protein levels are also increased by 1.5-fold 4 hr after R1881 addition (Figure 6B, upper panel). Consistently, overexpression of *Nkx3.1* leads to increased p53 protein levels without changing of its mRNA level (Figure S4, upper panel), suggesting that NKX3.1 modulates p53 at the posttranscriptional level. Furthermore, *Nkx3.1* expression leads to an increase in p53 half-life from 21 min to 30 min in LNCaP cells (Figure 6B, lower panel). Similar results were also obtained when using the *Pten* null murine PTEN-CaP2 prostate cancer cell line (Figure S4, lower panel).

To determine whether NKX3.1 stabilizes p53 in a MDM2-dependent manner, we introduced *Nkx3.1* into *p53/Mdm2* double null ($p53^{-/-};Mdm2^{-/-}$) mouse embryonic fibroblasts (Jones et al., 1995). Without MDM2, NKX3.1 has no significant influence on p53 expression levels (Figure 6C, compare lanes 3 and 4). When cotransfected with a vector containing *Mdm2*, NKX3.1 expression partially reverses the increased p53 degradation brought about by *Mdm2* overexpression (Figure 6C, compare lanes 5 with 6), suggesting that NKX3.1 controls p53 half-life via a MDM2-dependent mechanism.

MDM2 nuclear translocation and stability are known to be controlled by AKT phosphorylation (Mayo and Donner, 2001;

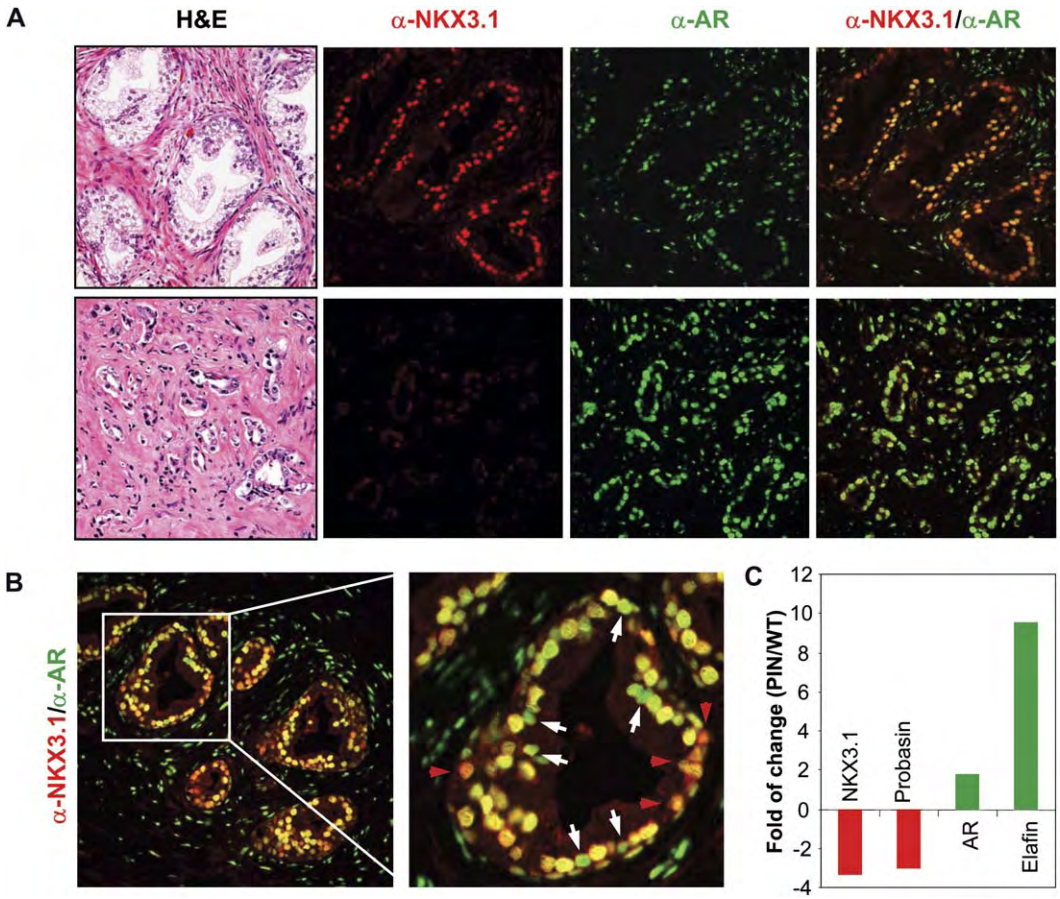

Figure 5. NKX3.1 controls AR level in human prostate cancers and modulates its target gene expression in *Pten* null prostate cancer model

A: Inverse correlation of NKX3.1 and AR levels in human prostate cancer samples. Representative images of double immunohistochemistry analysis using anti-NKX3.1 and AR antibodies.

B: Mosaic expression patterns of NKX3.1 and AR in human prostate samples. Double immunohistochemical analysis shows overlapping NKX3.1 and AR expression in most of the epithelial cells (in yellow), with some cells that have higher levels of either NKX3.1 (in red; red arrowheads) or AR (in green; white arrowheads) expression.

C: The relative expression levels of Nkx3.1, AR, and their target genes in *Pten*-deleted prostate glands. Microarray analysis was performed using mRNA prepared from the prostates of 6-week-old *Pten* null mice (PIN lesion stage) and their wild-type littermates (n = 5). Fold of changes in indicated genes was calculated as the relative expression levels of PIN versus wild-type ($p \leq 0.01$).

Zhou et al., 2001). To determine whether NKX3.1 antagonizes MDM2 function via an AKT-dependent mechanism, we treated PC3 cells with or without LY294002, a specific inhibitor for PI3K. As shown in Figure 6D, although P-AKT levels were significantly diminished, LY294002 treatment had no significant effect on either p53 (compare lanes 2 and 5) or NKX3.1-regulated p53 level (compare lanes 3 and 6). This result suggests that NKX3.1 regulates p53 half-life by modulating nuclear MDM2 activity, independent of AKT activation.

NKX3.1 can physically associate with HDAC1 and promotes p53 acetylation by recruiting HDAC1 from p53-MDM2-HDAC1 complex

Besides its E3 ubiquitin ligase activity, MDM2 can negatively regulate p53 half-life by recruiting a nuclear protein HDAC1, thereby promoting p53 deacetylation and degradation (Kobet et al., 2000; Ito et al., 2002; Brooks and Gu, 2003). To determine if enhanced p53 acetylation is one of the mechanisms involved in NKX3.1-mediated p53 half-life control, we examined acetylated p53 levels without or with *Nkx3.1* overexpression and found that NKX3.1 indeed enhances p53 acetylation (Figure 6E, upper panel). In vivo, NKX3.1 can physically associate with either endogenous or exogenous HDAC1 (Figure 6E, middle and lower panels), suggesting that NKX3.1 can form a complex with HDAC1 and change p53 acetylation status. Furthermore, NKX3.1 cannot further increase p53 levels in the presence of TSA, an inhibitor for HDAC activity, suggesting that NKX3.1 indeed depends on HDAC activity to regulate p53 level (Figure S5).

We then tested whether NKX3.1 can recruit HDAC1 from p53-MDM2-HDAC1 complex. To do this, *Mdm2* was introduced into $p53^{-/-};Mdm2^{-/-}$ cells, without or with *Nkx3.1*, followed by measurement of the relative amount of p53 associating with HDAC1. It was observed that *Mdm2* expression leads to increased p53-HDAC1 association by 4-fold, resulting in decreased total p53 protein level (compare lanes 1 and 2 of Figure 6F). In contrast, coexpressing *Nkx3.1* reduces p53-HDAC1 association, partially rescuing MDM2-mediated p53 degradation (Figure 6F, compare lanes 2 and 3). Thus, NKX3.1 regulates p53 half-life, as least in part, by recruiting HDAC1

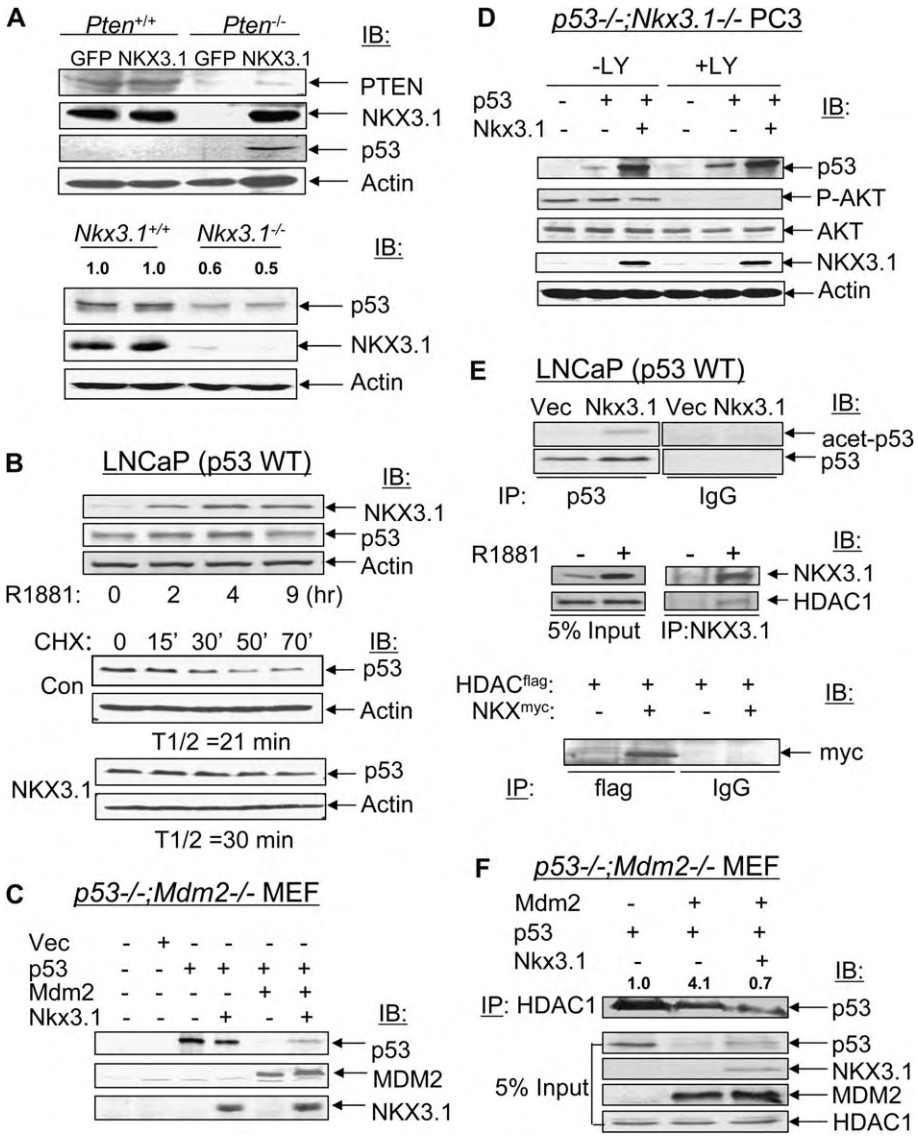

Figure 6. NKX3.1 regulates the level of p53 in a MDM2-dependent and AKT-independent manner

A: NKX3.1 regulates the level of p53 in vivo. Upper panel: reintroducing *Nkx3.1* into *Pten* null epithelium increases p53 protein level in regenerated grafts. Lower panel: knocking out *Nkx3.1* leads to decreased p53 protein levels. Cell lysates from *Nkx3.1* wild-type and null prostate tissues were analyzed using Western blot and normalized to actin loading control.

B: NKX3.1 regulated p53 level and half-life. Upper panel shows androgen-induced NKX3.1 expression and p53 increase in LNCaP cells. Lower panel: *Nkx3.1*-transfected LNCaP cells were incubated with cycloheximide for the indicated time, and total proteins were analyzed by Western blot. p53 half-life was calculated using Quantity One (Bio-Rad).

C: NKX3.1 stabilizes p53 via MDM2-dependent mechanism. Western blot analysis of cell lysates from $p53^{-/-};Mdm2^{-/-}$ MEFs after transfection of indicated plasmids.

D: NKX3.1 stabilizes p53 in an AKT-independent manner. PC3 cells were transfected with indicated plasmids with or without LY treatment before harvesting. Cell lysates were analyzed by Western blot.

E: NKX3.1 increases p53 acetylation and can physically associate with HDAC1. Upper panel: LNCaP cells were transfected without or with *Nkx3.1*, and the cell lysates were first immunoprecipitated with anti-p53 antibody and then blotted with antibodies recognizing either acetylated p53 or total p53, respectively. Middle panel: LNCaP cells were treated with androgen analog R1881 for 4–6 hr to induce *Nkx3.1* expression, and cell lysates were immunoprecipitated with anti-NKX3.1 antibody and then blotted with indicated antibodies. Lower panel: LNCaP cells were cotransfected with Flag-tagged HDAC1 and myc-tagged NKX3.1. Cell lysates were immunoprecipitated with either anti-Flag or control IgG and blotted with anti-myc antibody.

F: NKX3.1 modulates the level of p53 by recruiting HDAC1 from the MDM2-p53 complex. PC3 cells were cotransfected with indicated plasmid. Cell lysates were immunoprecipitated with anti-HDAC1 antibody and blotted with anti-p53 antibody. The relative amounts of p53 within the p53-HDAC1-MDM2 complex, as indicated above the Western blot, were calculated as HDAC1-associated p53:total p53 from the input, then normalized against lane 1.

from the HDAC1-MDM2-p53 complex, thereby promoting p53 acetylation.

Discussion

The involvement of NKX3.1 in human prostate cancer development has been intensively studied since its cloning (for review see Abdulkadir, 2005). Despite strong correlation of loss of NKX3.1 expression in human prostate cancer initiation and progression, several outstanding questions remain to be answered; these include but are not limited to the following. (1) How and at what level is NKX3.1 expression controlled in the prostate epithelium? (2) What is the normal function of NKX3.1 in vivo? And (3) what are the targets of NKX3.1, and how do those targets, upon NKX3.1 loss, contribute to prostate cancer initiation and progression? Our current study suggests that PTEN and its controlled signal pathway regulate NKX3.1 expression in the prostatic epithelium. Within the prostate epithelium, AR and NKX3.1 form a signaling feedback loop in which NKX3.1 is the negative modulator that keeps AR level and AR-controlled pathways in check. NKX3.1 regulates prostate cell proliferation and survival not only via its transcription factor activity, i.e., by negatively modulating the AR promoter, but also through protein-protein interaction with HDAC1 and consequently regulating p53 half-life and activity (Figure 7). Our finding emphasizes the cooperative effects between ubiquitously expressed *PTEN* tumor suppressor genes and prostatic-specific expressed *NKX3.1* in prostate cancer development.

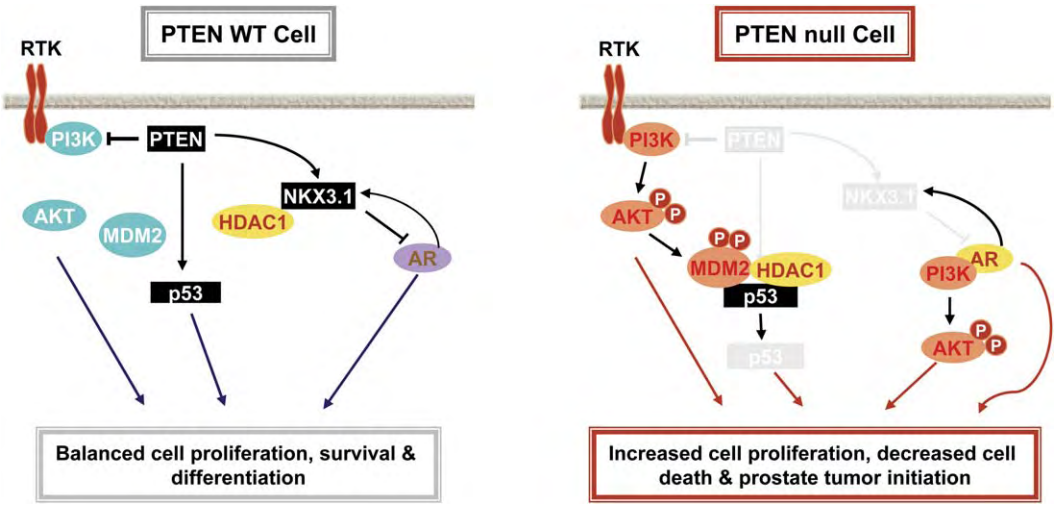

Figure 7. A schematic diagram illustrating the involvement of NKX3.1 in PTEN-controlled prostate tumorigenesis

In *Pten* wild-type prostatic epithelium (left panel), PTEN negatively regulates PI3K/AKT pathway but positively modulates p53 level and activity. The transcription level of *Nkx3.1* is controlled predominantly by PTEN as well as by AR. NKX3.1 in turn negatively regulates AR promoter activity and keeps AR and AR-controlled pathway in check. NKX3.1 also binds HDAC1 and releases p53 from p53-MDM2-HDAC1 complex, promoting p53 acetylation and activity. The net result of these NKX3.1-mediated PTEN functions is the balanced cell proliferation, differentiation, and cell death, which prevents prostate cancer initiation. Upon PTEN loss (right panel), the balance is broken, and NKX3.1 and its controlled signaling pathways are severely downregulated. AR, no longer under the control of NKX3.1, becomes overexpressed and activates its targets and downstream pathways, including PI3K/AKT pathway. In the absence of NKX3.1, most of the p53 is in the MDM2-HDAC1 complex, leading to p53 degradation. Activation of PI3K/AKT pathway, together with downregulated p53 activity and increased AR level and activity, leads to increased cell proliferation, decreased cell death, and prostate cancer initiation.

Several mechanisms have been proposed for loss of NKX3.1 expression in human prostate cancers, including both posttranscriptional modification, such as protein degradation, as well as transcriptional and epigenetic regulation (Asatiani et al., 2005; Bowen et al., 2000; He et al., 1997; Korkmaz et al., 2004; Ornstein et al., 2001; Voeller et al., 1997). The facts that NKX3.1 mRNA (Figure 5C and Wang et al., 2003) and protein levels (Figure 1A and Wang et al., 2003) are concomitantly downregulated in the *Pten* null prostate, and we can successfully restore *Nkx3.1* expression using an exogenous promoter and maintain near wild-type levels of NKX3.1 in different cell lines and in the renal capsule grafts (Figure 2C), suggest that PTEN modulates NKX3.1 function largely through regulation of its promoter activity. This conclusion is consistent with the strong correlation of NKX3.1 mRNA and protein levels in human prostate cancer specimens reported by a recent study (Korkmaz et al., 2004).

Nkx3.1 is positively regulated by androgen and its receptor AR at the transcriptional level (Bieberich et al., 1996; He et al., 1997; Magee et al., 2003; Prescott et al., 1998). Our results suggest that PTEN either predominantly controls NKX3.1 transcription or contributes significantly to AR-controlled mechanism. In the presence of PTEN, *Nkx3.1* expression can be modulated by AR, while in its absence, *Nkx3.1* expression is almost completely silenced despite increases in AR levels in *Pten* null prostate cancers (Wang et al., 2003; Figures 1A, 5C, and 7). Mechanisms involving enhancer/promoter and transcription activator/repressor interactions, epigenetic changes such as DNA methylation (Asatiani and Gelmann, 2005), and histone modification (Plass, 2002) are all potential possibilities by which NKX3.1 and AR interact and are regulated by PTEN and warrant a separate and more elaborate study.

Recently, Magee et al. identified NKX3.1 target genes that are sensitive to NKX3.1 dosage in a stochastic manner and, at the same time, are influenced by the androgen status in vivo (Magee et al., 2003). Among those target genes is a set regulated by androgens only in the absence of NKX3.1, suggesting that NKX3.1 functions as a selector for modulation of the expression of potential androgen target genes. We demonstrate that NKX3.1 loss, in either human prostate cancer samples (Figure 5A) or murine prostates of *Pten* and *Nkx3.1* knockout mice (Figures 5C and 4C), leads to increased AR levels. Conversely, overexpression of *Nkx3.1* decreases AR mRNA and protein expression (Figures 4A and 4D). These results imply that NKX3.1 is a negative regulator for AR expression, and AR and NKX3.1 form a feedback loop important for both prostate development and cancer formation. With *Nkx3.1* at steady-state levels, androgen/AR induces NKX3.1 expression, which in turn inhibits AR expression. Interestingly, the mosaic expression pattern of NKX3.1/AR target genes showed by Magee and colleagues (Magee et al., 2003) are similar to NKX3.1 and AR expression patterns observed in human prostate samples (Figure 5B), suggesting that the balance of NKX3.1-AR expression may ultimately determine the levels of target gene expression. The natural "set point" of this feedback loop and its range of action are currently unknown and require further investigation. Loss of NKX3.1 in the prostatic epithelium will impair this feedback system (Figure 7), which in turn leads to AR overexpression and may contribute to PIN lesion in *Nkx3.1* knockout mice (Abdulkadir et al., 2002; Kim et al., 2002a) and prostate cancer development in *Pten* null model (Wang et al., 2003), similar to what has been concluded from AR transgenic animals (Stanbrough et al., 2001) and human prostate cancer studies (Chen et al., 2004).

The growth-suppressive activities of NKX3.1 have been demonstrated in vitro in cell culture system and in vivo in knockout mice (Bhatia-Gaur et al., 1999; Kim et al., 2002a; Schneider et al., 2000; Tanaka et al., 2000). NKX3.1 haploinsufficiency or

loss leads to significant delay in exiting from the cell cycle (Magee et al., 2003), but how NKX3.1 engages the cell cycle machinery to regulate prostatic epithelium growth is currently unknown. Here, we showed that restoration of *Nkx3.1* expression to the wild-type level in *Pten* null prostatic epithelium leads to increased p53 protein levels in vivo and in vitro. NKX3.1 can physically associate with HDAC1 and recruit HDAC1 from the HDAC1-MDM2-p53 complex, protecting p53 from deacetylation and degradation. Furthermore, NKX3.1 stabilizes p53 through modulation of MDM2 activity in the nucleus, independent of AKT-mediated MDM2 phosphorylation and nuclear translocation. Whether the above-mentioned pathways involve or collaborate with NKX3.1-regulated oxidative damage or p53-dependent senescence requires further investigation (Chen et al., 2005; Ouyang et al., 2005).

Although this study suggests that NKX3.1 plays an essential role in PTEN-controlled prostate cancer development, NKX3.1 loss alone only mimics a part of *Pten* deletion phenotype, suggesting that other PTEN-controlled pathways may synergistically interact with those NKX3.1-dependent events (Figure 7). AKT hyperphosphorylation has been observed in isolated clusters of cells within regions of high grade PIN lesions in *Nkx3.1*$^{+/-}$ and *Nkx3.1*$^{-/-}$ mice, and deletion of one allele of *Pten* in *Nkx3.1* null mice leads to accelerated tumor initiation and increased incidence of high-grade PIN (Kim et al., 2002b). However, differing from the *Pten* null prostate cancer model (Wang et al., 2003), *Pten*$^{+/-}$*;Nkx3.1*$^{-/-}$ mice do not progress to metastatic prostate cancer (Kim et al., 2002b). These results suggest that the dosage of PTEN plays a dominant role in the cooperative effect of NKX3.1 and PTEN.

We showed that forced *Nkx3.1* expression in *Pten* null epithelium significantly induces cell apoptosis in the mutant grafts. This mechanism, together with NKX3.1's growth suppression function, leads to reduced graft size. Interestingly, the effects of NKX3.1 appear to depend on the PTEN status: *Nkx3.1* overexpression leads to increased cell death and decreased cell proliferation in the *Pten* null grafts but has no significant impact on the wild-type grafts. One possible explanation is that *Pten* null cells have become "addicted" to high levels of PI3K/AKT activity and, consequently, are hypersensitive to inhibition of this pathway. We have previously shown that PTEN-deficient human cancer cell lines and murine *Pten* null tumors are sensitive to inhibitors specific for mTOR, a downstream effector of the PI3K/AKT pathway (Neshat et al., 2001). In the present study, we demonstrate that NKX3.1 inhibits AKT phosphorylation/activation via an AR-dependent mechanism and show that NKX3.1 expression in vivo can block the hyperproliferative and antiapoptotic effects brought on by PTEN loss. This mechanism elucidates a pathway that can potentially be targeted with specific therapies for human prostate cancer, given that 30% of primary prostate cancers and as many as 60% of metastatic cases exhibit *PTEN* LOH (Sellers and Sawyers, 2002).

Experimental procedures

Immunohistochemical analysis

Tissues were fixed in 10% buffered Formalin for 6 hr, followed by transfer to 70% alcohol. These paraffin-embedded tissues were sectioned (4 μm) and stained with hematoxylin and eosin. Antigen retrieval was performed by incubating the slides in 0.01 M citric acid buffer (pH 6.0) at 95°C for 30 min. The endogenous peroxidase activity was inactivated in a solution containing 3% hydrogen peroxide (H_2O_2) in methanol. The following detection and visualization procedures were performed according to the manufacturer's protocol. Negative control slides were performed without primary antibody. Control slides known to be positive for each antibody were incorporated. For fluorescence double staining, pretreated sections were first blocked with mouse Ig blocking reagent in the VECTOR M.O.M. Immunodetection Kit (Vector Laboratories) and then incubated with mouse antibody PTEN (26H9, Cell Signaling Technology), Ki67 (NCL-Ki67-MM1), or NKX3.1 (a kind gift from Dr. Abate-Shen) at room temperature for 30 min, followed by signal amplification with TSA Plus Fluorescence Systems (PerkinElmer). After biotin blocking, the section was then stained with rabbit antibody P-AKT (9277, Cell Signaling Technology) or AR (PG21, Upstate), and signal was amplified with TSA system with different fluorescence. For human prostate tissue array, PTEN, NKX3.1 (SC-816 and SC-15022, Santa Cruz), and AR (PG21, Upstate) were used.

Tissue array analysis

Double immunofluorescent staining was performed as above. PTEN and NKX3.1 (Santa Cruz SC-816 and SC-15022, respectively) intensity was analyzed by Image Plus software, and only cores with epithelial structure were chosen for further analysis. Briefly, we chose four views for each core; measured the signal intensity using Image Plus software; and signed the signal intensity as 0–6, in which 0[<50]; 1[50-75]; 2[75–100]; 3[100–125]; 4[125–150]; 5[150–175]; 6[>175]. According to the average intensity value, samples were categorized into grades. By using the intensity grade, a stacked line was generated with value of each sample displayed. Linear regression analysis was performed for the correlation between PTEN and NKX3.1 expression by SPSS software and presented as Skattergram.

Preparation of prostate epithelial cells, virus infection, and prostate regeneration

Four- and six-week-old *Pten* wild-type and mutant mice were killed by carbon dioxide inhalation. Prostates were dissected, cut into small pieces with a steel blade, and digested with 0.8 mg/ml collagenase (GIBCO, 226 units/mg) in 10 ml of DMEM 10% FBS (GIBCO) at 37°C for 90 min. Cells were filtered through 100 μm nylon mesh (Becton Dickinson), washed twice with 10 ml of DMEM 10% FBS, resuspended in 1 ml of DMEM 10% FBS, and counted.

The lentivirus was prepared as described (Lois et al., 2002; Pfeifer et al., 2002). Infection was carried out according to Xin et al. (2003). Briefly, 1 × 10^5 prostate cells were mixed with GFP or NKX3.1 Lentivirus stock (titer 2 × 10^7) in the presence of 8 μg/ml polybrene (Sigma), then centrifuged at 1500 rpm with a Beckman GS-6R centrifuge (Beckman Coulter) for 2 hr at room temperature and washed twice with 1 ml of DMEM 10% FBS. All procedures were performed under University of California Los Angeles safety regulations for lentivirus usage.

Mouse prostate regeneration was performed according to previous reports (Cunha and Donjacour, 1987; Thompson et al., 1989; Xin et al., 2003). Lentivirus-infected cells (1 × 10^5) were combined with UGSM cells (1 × 10^5) and 25 μl of type I collagen (Roche) and then grafted under the renal capsule. Each experiment contained grafts of UGSM alone to ensure that tissue growth did not result from contaminating urogenital sinus epithelial cells. Grafts were harvested and weighed after 6–9 weeks. All surgical procedures were performed under Division of Laboratory Animal Medicine regulations of the University of California, Los Angeles.

Cell proliferation and apoptosis index

Cell proliferation index was examined by Ki67 staining. Five different fields were chosen, and then 200 cells were counted in each field. Ki67+ cells were presented as the percentage of nucleated cells. Cell apoptosis were determined by TUNEL assay using the In Situ Cell Death Detection Kit from Roche according to the manufacturer's instruction. Sections were dewaxed with xylene and rehydrated through graded alcohol. DNA fragmentation was labeled with fluorescein-conjugated dUTP and visualized with fluorescence. TUNEL-positive cells were counted and presented the percentage of nucleated cells.

Western blot analysis

Protein lysate was prepared by sonicating graft tissues and prostate tissue from *Nkx3.1* mice, R1881 treated or transfected LNCaP, PC3 and PTEN-CaP2 cells in buffer containing 50 mM Tris-HCl (pH 8.0), 150 mM NaCl,

0.1% SDS, 0.5% SD, 1% NP-40, 1 mM EDTA, 1 mM PMSF, 25 mM NaF, and cocktail protease inhibitors (Roche). Tissue lysate (40 μg) was resolved to SDS-PAGE followed by Western blot analysis using anti-p53 (Ab-1, Oncogene; DO-1, Santa Cruz), P-AKT (9271, Cell Signaling), total AKT (Cell Signaling), NKX3.1 (SC-15022, Santa Cruz), MDM2 (Ab-2, Oncogene), Flag (Stratagene), and Actin (#5060, Sigma) antibodies, respectively.

For immunoprecipitation experiments, 500 μg of cell lysate was incubated 16 hr at 4°C with 2 μg AR or p85α antibody (PG-21 and #06-496, Upstate), p53 antibody (DO-1, Santa Cruz), NKX3.1 or HDAC1 (SC-15022, SC-07872, Santa Cruz), or Flag antibody (Sigma, F1804) plus 50 μl Protein A agarose beads (#16-125, Upstate). Beads were washed three times with lysis buffer and centrifuged for 5 min at 5000 g between each wash. Protein was eluted from beads with 50 μl Laemmli sample buffer (Bio-Rad). Lysates were resolved on a 10% SDS-PAGE gel and transferred onto nitrocellulose (Bio-Rad).

For endogenous NKX3.1 induction, LNCaP cells were treated with 2 nM R1881 for different time periods after being plated in 10% charcoal serum for 2 days. For half-life experiments, *NKX3.1* was transfected into LNCaP cells 36 hr prior to the addition of 50 μg/ml cycloheximide (Cycloheximide, Calbiochem) in serum-free medium. Cells were then lysed at indicated time points and further analyzed by Western blot.

Supplemental data

The Supplemental Data include Supplemental Experimental Procedures and five supplemental figures and can be found with this article online at http://www.cancercell.org/cgi/content/full/9/5/367/DC1/.

Acknowledgments

We thank Drs. David Mulholland, Charles Sawyers, Yue Xiong, Kunliang Guan, Xuan Liu, Joseph Lasky, and George Thomas and colleagues in the Wu and Witte laboratories for helpful comments and suggestions; Dr. Mary Perry for Mdm2 plasmid; Dr. Edward P. Gelmann for human NKX3.1 plasmid; Dr. Cory Abate-Shen for NKX3.1 antibody and depositing NKX3.1 knockout mice in the MMHCC/NCI mouse cancer model repository; John Wongvipat from Dr. Charles Sawyers' laboratory for providing *Nkx3.1* knockout mice; Drs. Gang Wang and Feng Xu for advice in ChIP analysis; and PDL, Dr. Graeber, and Ms. Bhopale for microarray analysis. Q.L. is supported by the seed grant from the UCLA'S Jonsson Cancer Center Foundation. J.J. is supported by the DOD postdoctoral fellowship. O.N.W. is an investigator of the Howard Hughes Medical Institute. This work is partly supported by funds from DOD PC031130 and NCI UO1 CA84128-06 and RO1 CA107166 (for H.W.) and Prostate Cancer Foundation and NCI P50 CA092131 SPORE (for O.N.W.).

Received: September 30, 2005
Revised: March 1, 2006
Accepted: March 22, 2006
Published: May 15, 2006

References

Abdulkadir, S.A. (2005). Mechanisms of prostate tumorigenesis: Roles for transcription factors Nkx3.1 and Egr1. Ann. NY Acad. Sci. *1059*, 33–40 10.1196/annals.1339.018.

Abdulkadir, S.A., Magee, J.A., Peters, T.J., Kaleem, Z., Naughton, C.K., Humphrey, P.A., and Milbrandt, J. (2002). Conditional loss of Nkx3.1 in adult mice induces prostatic intraepithelial neoplasia. Mol. Cell. Biol. *22*, 1495–1503.

Asatiani, E., and Gelmann, E.P. (2005). Targeted therapies for prostate cancer. Expert Opin. Ther. Targets *9*, 283–298.

Asatiani, E., Huang, W.-X., Wang, A., Rodriguez Ortner, E., Cavalli, L.R., Haddad, B.R., and Gelmann, E.P. (2005). Deletion, methylation, and expression of the NKX3.1 suppressor gene in primary human prostate cancer. Cancer Res. *65*, 1164–1173. 10.1158/0008–5472.CAN-04–2688.

Baron, S., Manin, M., Beaudoin, C., Leotoing, L., Communal, Y., Veyssiere, G., and Morel, L. (2004). Androgen receptor mediates non-genomic activation of phosphatidylinositol 3-OH kinase in androgen-sensitive epithelial cells. J. Biol. Chem. *279*, 14579–14586.

Bhatia-Gaur, R., Donjacour, A.A., Sciavolino, P.J., Kim, M., Desai, N., Young, P., Norton, C.R., Gridley, T., Cardiff, R.D., Cunha, G.R., et al. (1999). Roles for Nkx3.1 in prostate development and cancer. Genes Dev. *13*, 966–977.

Bieberich, C.J., Fujita, K., He, W.W., and Jay, G. (1996). Prostate-specific and androgen-dependent expression of a novel homeobox gene. J. Biol. Chem. *271*, 31779–31782.

Bowen, C., Bubendorf, L., Voeller, H.J., Slack, R., Willi, N., Sauter, G., Gasser, T.C., Koivisto, P., Lack, E.E., Kononen, J., et al. (2000). Loss of NKX3.1 expression in human prostate cancers correlates with tumor progression. Cancer Res. *60*, 6111–6115.

Brooks, C.L., and Gu, W. (2003). Ubiquitination, phosphorylation and acetylation: the molecular basis for p53 regulation. Curr. Opin. Cell Biol. *15*, 164–171.

Chen, C.D., Welsbie, D.S., Tran, C., Baek, S.H., Chen, R., Vessella, R., Rosenfeld, M.G., and Sawyers, C.L. (2004). Molecular determinants of resistance to antiandrogen therapy. Nat. Med. *10*, 33–39.

Chen, Z., Trotman, L.C., Shaffer, D., Lin, H.K., Dotan, Z.A., Niki, M., Koutcher, J.A., Scher, H.I., Ludwig, T., Gerald, W., et al. (2005). Crucial role of p53-dependent cellular senescence in suppression of Pten-deficient tumorigenesis. Nature *436*, 725–730.

Cunha, G.R., and Donjacour, A. (1987). Mesenchymal-epithelial interactions: technical considerations. Prog. Clin. Biol. Res. *239*, 273–282.

Dahia, P.L. (2000). PTEN, a unique tumor suppressor gene. Endocr. Relat. Cancer *7*, 115–129.

DeMarzo, A.M., Nelson, W.G., Isaacs, W.B., and Epstein, J.I. (2003). Pathological and molecular aspects of prostate cancer. Lancet *361*, 955–964.

Di Cristofano, A., De Acetis, M., Koff, A., Cordon-Cardo, C., and Pandolfi, P.P. (2001). Pten and p27KIP1 cooperate in prostate cancer tumor suppression in the mouse. Nat. Genet. *27*, 222–224.

Freeman, D.J., Li, A.G., Wei, G., Li, H.H., Kertesz, N., Lesche, R., Whale, A.D., Martinez-Diaz, H., Rozengurt, N., Cardiff, R.D., et al. (2003). PTEN tumor suppressor regulates p53 protein levels and activity through phosphatase-dependent and -independent mechanisms. Cancer Cell *3*, 117–130.

Gregorakis, A.K., Holmes, E.H., and Murphy, G.P. (1998). Prostate-specific membrane antigen: current and future utility. Semin. Urol. Oncol. *16*, 2–12.

Hanahan, D., and Weinberg, R.A. (2000). The hallmarks of cancer. Cell *100*, 57–70.

He, W.W., Sciavolino, P.J., Wing, J., Augustus, M., Hudson, P., Meissner, P.S., Curtis, R.T., Shell, B.K., Bostwick, D.G., Tindall, D.J., et al. (1997). A novel human prostate-specific, androgen-regulated homeobox gene (NKX3.1) that maps to 8p21, a region frequently deleted in prostate cancer. Genomics *43*, 69–77.

Ito, A., Kawaguchi, Y., Lai, C.H., Kovacs, J.J., Higashimoto, Y., Appella, E., and Yao, T.P. (2002). MDM2-HDAC1-mediated deacetylation of p53 is required for its degradation. EMBO J. *21*, 6236–6245.

Jones, S.N., Roe, A.E., Donehower, L.A., and Bradley, A. (1995). Rescue of embryonic lethality in Mdm2-deficient mice by absence of p53. Nature *378*, 206–208.

Kim, M.J., Bhatia-Gaur, R., Banach-Petrosky, W.A., Desai, N., Wang, Y., Hayward, S.W., Cunha, G.R., Cardiff, R.D., Shen, M.M., and Abate-Shen, C. (2002a). Nkx3.1 mutant mice recapitulate early stages of prostate carcinogenesis. Cancer Res. *62*, 2999–3004.

Kim, M.J., Cardiff, R.D., Desai, N., Banach-Petrosky, W.A., Parsons, R., Shen, M.M., and Abate-Shen, C. (2002b). Cooperativity of Nkx3.1 and Pten loss of function in a mouse model of prostate carcinogenesis. Proc. Natl. Acad. Sci. USA *99*, 2884–2889.

Kobet, E., Zeng, X., Zhu, Y., Keller, D., and Lu, H. (2000). MDM2 inhibits p300-mediated p53 acetylation and activation by forming a ternary complex with the two proteins. Proc. Natl. Acad. Sci. USA *97*, 12547–12552.

Korkmaz, C.G., Korkmaz, K.S., Manola, J., Xi, Z., Risberg, B., Danielsen, H., Kung, J., Sellers, W.R., Loda, M., and Saatcioglu, F. (2004). Analysis of

androgen regulated homeobox gene NKX3.1 during prostate carcinogenesis. J. Urol. *172*, 1134–1139.

Lois, C., Hong, E.J., Pease, S., Brown, E.J., and Baltimore, D. (2002). Germline transmission and tissue-specific expression of transgenes delivered by lentiviral vectors. Science *295*, 868–872.

Ma, X., Ziel-van der Made, A.C., Autar, B., van der Korput, H.A., Vermeij, M., van Duijn, P., Cleutjens, K.B., de Krijger, R., Krimpenfort, P., Berns, A., et al. (2005). Targeted biallelic inactivation of Pten in the mouse prostate leads to prostate cancer accompanied by increased epithelial cell proliferation but not by reduced apoptosis. Cancer Res. *65*, 5730–5739.

Maehama, T., Taylor, G.S., and Dixon, J.E. (2001). PTEN and myotubularin: novel phosphoinositide phosphatases. Annu. Rev. Biochem. *70*, 247–279.

Magee, J.A., Abdulkadir, S.A., and Milbrandt, J. (2003). Haploinsufficiency at the Nkx3.1 locus. A paradigm for stochastic, dosage-sensitive gene regulation during tumor initiation. Cancer Cell *3*, 273–283.

Mayo, L.D., and Donner, D.B. (2001). A phosphatidylinositol 3-kinase/Akt pathway promotes translocation of Mdm2 from the cytoplasm to the nucleus. Proc. Natl. Acad. Sci. USA *98*, 11598–11603.

McDavid, K., Lee, J., Fulton, J.P., Tonita, J., and Thompson, T.D. (2004). Prostate cancer incidence and mortality rates and trends in the United States and Canada. Public Health Rep. *119*, 174–186.

Neshat, M.S., Mellinghoff, I.K., Tran, C., Stiles, B., Thomas, G., Petersen, R., Frost, P., Gibbons, J.J., Wu, H., and Sawyers, C.L. (2001). Enhanced sensitivity of PTEN-deficient tumors to inhibition of FRAP/mTOR. Proc. Natl. Acad. Sci. USA *98*, 10314–10319.

Ornstein, D.K., Cinquanta, M., Weiler, S., Duray, P.H., Emmert-Buck, M.R., Vocke, C.D., Linehan, W.M., and Ferretti, J.A. (2001). Expression studies and mutational analysis of the androgen regulated homeobox gene NKX3.1 in benign and malignant prostate epithelium. J. Urol. *165*, 1329–1334.

Ouyang, X., DeWeese, T.L., Nelson, W.G., and Abate-Shen, C. (2005). Loss-of-function of Nkx3.1 promotes increased oxidative damage in prostate carcinogenesis. Cancer Res. *65*, 6773–6779.

Parson, W., Parsons, T.J., Scheithauer, R., and Holland, M.M. (1998). Population data for 101 Austrian Caucasian mitochondrial DNA d-loop sequences: application of mtDNA sequence analysis to a forensic case. Int. J. Legal Med. *111*, 124–132.

Pfeifer, A., Ikawa, M., Dayn, Y., and Verma, I.M. (2002). Transgenesis by lentiviral vectors: lack of gene silencing in mammalian embryonic stem cells and preimplantation embryos. Proc. Natl. Acad. Sci. USA *99*, 2140–2145.

Plass, C. (2002). Cancer epigenomics. Hum. Mol. Genet. *11*, 2479–2488.

Prescott, J.L., Blok, L., and Tindall, D.J. (1998). Isolation and androgen regulation of the human homeobox cDNA, NKX3.1. Prostate *35*, 71–80.

Rocchi, P., So, A., Kojima, S., Signaevsky, M., Beraldi, E., Fazli, L., Hurtado-Coll, A., Yamanaka, K., and Gleave, M. (2004). Heat shock protein 27 increases after androgen ablation and plays a cytoprotective role in hormone-refractory prostate cancer. Cancer Res. *64*, 6595–6602.

Schneider, A., Brand, T., Zweigerdt, R., and Arnold, H. (2000). Targeted disruption of the Nkx3.1 gene in mice results in morphogenetic defects of minor salivary glands: parallels to glandular duct morphogenesis in prostate. Mech. Dev. *95*, 163–174.

Sellers, W., and Sawyers, C. (2002). Somatic Genetics of Prostate Cancer: Oncogene and Tumor Suppressors (Philadelphia: Lippincott Williams & Wilkins).

Stanbrough, M., Leav, I., Kwan, P.W., Bubley, G.J., and Balk, S.P. (2001). Prostatic intraepithelial neoplasia in mice expressing an androgen receptor transgene in prostate epithelium. Proc. Natl. Acad. Sci. USA *98*, 10823–10828.

Sun, M., Yang, L., Feldman, R.I., Sun, X.M., Bhalla, K.N., Jove, R., Nicosia, S.V., and Cheng, J.Q. (2003). Activation of phosphatidylinositol 3-kinase/Akt pathway by androgen through interaction of p85α, androgen receptor, and Src. J. Biol. Chem. *278*, 42992–43000.

Suzuki, H., Freije, D., Nusskern, D.R., Okami, K., Cairns, P., Sidransky, D., Isaacs, W.B., and Bova, G.S. (1998). Interfocal heterogeneity of PTEN/MMAC1 gene alterations in multiple metastatic prostate cancer tissues. Cancer Res. *58*, 204–209.

Tanaka, M., Komuro, I., Inagaki, H., Jenkins, N.A., Copeland, N.G., and Izumo, S. (2000). Nkx3.1, a murine homolog of Drosophila bagpipe, regulates epithelial ductal branching and proliferation of the prostate and palatine glands. Dev. Dyn. *219*, 248–260.

Thompson, T.C., Southgate, J., Kitchener, G., and Land, H. (1989). Multistage carcinogenesis induced by ras and myc oncogenes in a reconstituted organ. Cell *56*, 917–930.

Trotman, L.C., Niki, M., Dotan, Z.A., Koutcher, J.A., Di Cristofano, A., Xiao, A., Khoo, A.S., Roy-Burman, P., Greenberg, N.M., Van Dyke, T., et al. (2003). Pten dose dictates cancer progression in the prostate. PLoS Biol. *1*, e59. 10.1371/journal.pbio.0000059.

Vivanco, I., and Sawyers, C.L. (2002). The phosphatidylinositol 3-Kinase AKT pathway in human cancer. Nat. Rev. Cancer *2*, 489–501.

Voeller, H.J., Augustus, M., Madike, V., Bova, G.S., Carter, K.C., and Gelmann, E.P. (1997). Coding region of NKX3.1, a prostate-specific homeobox gene on 8p21, is not mutated in human prostate cancers. Cancer Res. *57*, 4455–4459.

Wang, S., Gao, J., Lei, Q., Rozengurt, N., Pritchard, C., Jiao, J., Thomas, G.V., Li, G., Roy-Burman, P., Nelson, P.S., et al. (2003). Prostate-specific deletion of the murine Pten tumor suppressor gene leads to metastatic prostate cancer. Cancer Cell *4*, 209–221.

Xin, L., Ide, H., Kim, Y., Dubey, P., and Witte, O.N. (2003). In vivo regeneration of murine prostate from dissociated cell populations of postnatal epithelia and urogenital sinus mesenchyme. Proc. Natl. Acad. Sci. USA *100* (*Suppl 1*), 11896–11903.

Xin, L., Lawson, D.A., and Witte, O.N. (2005). The Sca-1 cell surface marker enriches for a prostate-regenerating cell subpopulation that can initiate prostate tumorigenesis. Proc. Natl. Acad. Sci. USA *102*, 6942–6947.

Zhou, B.P., Liao, Y., Xia, W., Zou, Y., Spohn, B., and Hung, M.C. (2001). HER-2/neu induces p53 ubiquitination via Akt-mediated MDM2 phosphorylation. Nat. Cell Biol. *3*, 973–982.

Novel Murine Prostate Cancer Cell Lines Provide Insight into PTEN's Dosage Effect on tumorigenesis and Androgen Responsiveness

Jing Jiao[1], Shunyou Wang[1], Rong Qiao[1], Igor Vivanco[1], Philip A. Watson[2], Charles L. Sawyers[1,2,3], Hong Wu[1*]

[1]Department of Molecular and Medical Pharmacology, [2]Department of Medicine, and [3]Howard Hughes Medical Institute, University of California at Los Angeles, CA 90095-1735

*Correspondence:
Dr. Hong Wu
Department of Molecular and Medical Pharmacology
UCLA School of Medicine
650 CE Young Drive South
Los Angeles, CA 90095-1735
Phone: 310-825-5160
Fax: 310-267-0242
Email: **hwu@mednet.ucla.edu**

Running title: Critical role of PTEN in hormone refractory prostate cancer formation

Key words: PTEN, AR, tumorigenesis, HRPC, novel murine prostate cancer cell lines

Abstract

PTEN mutations are among the most frequent genetic alterations found in human prostate cancers. Our previous works suggest that the onset and progression of prostate cancer development depend on the PTEN dosage: while precancerous lesions were found in *Pten* heterozygous mice, cancer progression and metastasis only happened when both alleles of *Pten* were deleted. To understand the molecular mechanisms underlying PTEN's dosage effects, we have generated two pairs of isogenic, androgen receptor (AR) positive prostate epithelial lines from hormone naïve *Pten* knockout mice that are either heterozygous (PTEN-P2 and –P8) or homozygous (PTEN-CaP2 and –CaP8) for *Pten* deletion. Despite no prior exposure to hormone ablation therapy, *Pten* null cells are tumorigenic on both male and female SCID mice, suggesting that PTEN intrinsically controls androgen responsiveness, a critical step in the development of hormone refractory prostate cancer. Although PTEN haploinsufficiency renders cells acquire androgen independence, heterozygous *Pten* deletion by itself is not sufficient for tumorigenesis. Furthermore, bss of the second allele of *Pten* leads to a higher level of androgen receptor expression, accelerated cell cycle progression and anchorage-independent growth without obvious structural or numerical chromosome changes based on the SKY karyotyping analysis. Importantly, knocking down AR by shRNA in *Pten* null cells completely reverse cell cycle phenotype in vitro and partially rescue tumorigenesis in vivo, indicating that PTEN controlled prostate tumorigenesis is AR-dependent. These cell lines will serve as useful tools for understanding signaling pathways controlled by PTEN and elucidating the molecular mechanisms involved in hormone refractory prostate cancer formation.

Introduction

Prostate cancer is the second leading cause of cancer related death among North American men (1). Despite improved early detection and initial positive response to androgen ablation therapies, some patients eventually develop hormone refractory prostate cancer (HRPC). The molecular mechanisms leading to the progression of HRPC are still poorly understood (2) and proposed hypotheses ranging from gain of function mutations under hormone deprivation to intrinsic properties of certain prostate cancer cells (3).

Among genetic alterations frequently found in human prostate cancers, *PTEN* loss of function has been strongly implicated in the prostate cancer development (4, 5). The etiologic role of PTEN in prostate tumorigeneisis is further supported by studying animals models with prostate-specific deletion of its murine homology, the *Pten* gene (6-8). In contrast to conventional heterozygous *Pten* deletion (Freeman et al., 2006), conditional deletion of both alleles of *Pten* significantly reduced the latency of PIN lesion development from 10 months to 6 weeks. Importantly, *Pten* null animals progress from PIN to localized adenocarcinoma to metastasis with precise kinetics (7), suggesting that the onset and progression of prostate cancer is PTEN dosage dependent. Similar to majority of human prostate cancers, *Pten* null murine prostate cancer initially regress in response to androgen ablation therapy, but subsequently relapse and proliferate in the absence of androgens. Therefore, the *Pten* prostate cancer model provides an ideal system for studying the mechanism of HRPC.

Since most of well studied human prostate cancer cell lines are derived from late stage cancer samples after hormone ablation therapy and, therefore, are not hormone naïve and suitable for studying process involved in HRPC, we decided to establish primary cell lines from intact hormone naive *Pten* conditional knockout mice. Here, we report the establishment and characterization of two pairs of isogenic cell lines and their usage to address (1) whether prostatic epithelial cells can acquire androgen-independency without androgen deprivation, and (2) the relationship between loss of PTEN and androgen independence growth.

Materials and Methods

Establishment of primary cell lines from Pten prostate cancer model. Prostate cancer tissue was dissected from a 10 month adult mouse, minced, and digested with 0.5% collagenase type I. After filtrating through a 40um mesh, the fragments trapped by the mesh were plated in tissue culture dishes coated with type I collagen (BD Biosciences)(9). Several cell populations with distinct morphology were observed in the confluent monolayer developed from the tissue fragments. Areas of epithelial cells were collected and single cells plated into a 96-well plate. The PTEN-P2 and PTEN-P8 cell lines were established as a spontaneously immortalized line from one well each. The lines were maintained in DMEM supplemented with 10% fetal bovine serum (FBS; Omega Scientific, Tarzana, CA), 25ug/mL bovine pituitary extract, 5 ug/mL bovine insulin, and 6 ng/mL recombinant human epidermal growth factor (all from Sigma-Aldrich, St. Louis, MO). The PTEN-CaP2 and PTEN-CaP8 were generated by infecting PTEN-P2 or PTEN-P8 cell lines with Cre-retrovirus followed by 2 weeks of puromycin selection.

Real time PCR. Briefly, total RNAs from culture cells were extracted with RNeasy Micro kit (Qiagen, Valencia, CA). RNAs were reverse-transcribed into cDNA with SuperScript III First-Strand Synthesis System for qRT-PCR (Invitrogen) and Quantitative PCR was done in the iQ thermal cycler (Bio-Rad, Hercules, CA) using the iQ SYBR Green Supermix (Bio-Rad). Quantitative PCR for each sample was run in triplicate. Results were analyzed by the relative quantification method and expressed as relative RNA levels. The relative RNA level was then calculated by normalizing the ΔCT of each gene to the least abundant RNA species, which was arbitrarily set to 15. The relative RNA level of gene *x* is thus equal to 15 - ΔCT(*x*). All PCR primers were synthesized by Operon Biotechnologies (Huntsville, AL) and designed for the mouse sequence unless otherwise specified. The following primer pairs were used: AR forward, 5-AACCAACCAGATTCCTTTGC-3, reverse, ATTAGTGAAGGACCGCCAAC-3; CK5 forward, 5-ACCTTCGAAACACCAAGCAC-3, reverse, 5-TTGGCACACTGCTTCTTGAC-3; CK14 forward, 5-GACTTCCGGACCAAGTTTGA-3, reverse, 5-CCTTGAGGCTCTCAATCTGC-3; CK8 forward, 5-ATCGAGATCACCACCTACCG-3, reverse, 5-TGAAGCCAGGGCTAGTGAGT-3; CK18 forward, 5- ACTCCGCAAGGTGGTAGATG-3, reverse, 5-GCCTCGATTTCTGTCTCCAG-3; TAP63 forward, 5-GAAGGCAGATGAAGACAGCA-3, reverse, 5- GGAAGTCATCTGGATTCCGT-3; DNp63 forward, 5- TCTGATGGCATTTGACCCTA-3, reverse, 5-TACCAACAGATGGGAAGCAA-3; PSCA forward, 5-GCTGCTACTCTGACCTGTGC-3, reverse, 5- TTCACAATCGGGCTATGGTA-3; Nkx3.1 forward, 5- CGACTGAACCCGAGTCTGAT-3, reverse, 5-

ATGGCTGAACTTCCTCTCCA-3; CMA forward, 5-GGGAGCTGGAACATAAGCAG-3, reverse, 5-TGTCCTCCCATTCTCTGGAC-3; SPN forward, 5- CTTTGTGAAGGTGCTGCAAT, reverse, 5-GTCTTGTTGGCACAATCCAC-3.

Western analysis Protein lysate were prepared from confluent cells by adding RIPA buffer containing 50mM Tris-HCl (pH 8.0), 150mM NaCl, 0.1% SDS, 0.5% SD, 1% NP-40, 1mM EDTA, 1mM PMSF, 25mM NaF, cocktail protease inhibitors (Roche) and phosphatase inhibitors (sigma). 50 ug protein lysate were resolved on SDS-PAGE followed by Western blot analysis using anti-PTEN (9552, Cell Signaling), AR (N-20, Santa Cruz), p-AKT (9271, cell signaling), total AKT (9272, Cell signaling), Nkx3.1 (sc-15022, Santa Cruz), Cre (MAB3120, Chemicon), p21(sc-471, Santa Cruz), p27 (sc-1641, Santa Cruz), E-Cadherin (610181, BD bioscience) and Actin (5060, Sigma) antibodies, respectively.

Retroviral transduction Androgen receptor knockdown was achieved by infecting PTEN-CaP2 and PTEN-CaP8 cells with pSIREN-RetroQ-DsRed (pSRQ-R) retrovirus expressing shRNA. pSRQ-R is a retroviral RNAi vector containing red fluorescent protein (Clontech).

AR RNAi primer: 5'- GATCCGCGATTGTACCATTGATAAATTCAAGAGA TTTATCAATGGTACAATCG TTTTTTACGCGTG -3' and 5' TTAAGTGCGCATTTTTTGCTAACATGGTAACTATTTAGAGAACTTAAATAGTT ACCATGTTAGCGC -3'. The annealed oligos were cloned into the BamHI-ECoRI site

of pSRQ-R and positive clones were confirmed by sequencing. pSRQ-R /AR-RNAi or control vector containing negative RNAi (clontech) and ecotropical packaging plasmid were transfected into 293T packaging cells individually and the collected retrovirus was used to infect PTEN-CaP2 and PTEN-CaP8 cells. Cre recombinase virus was made by transfecting pMSCV-puro-Cre and ecotropic packaging plasmid into 293T cells.

In vitro cell growth assay To determine cell growth in Charcoal stripped serum (CCS) medium, cells were seeded into 6-well plates at $5x10^4$ cells/well in the maintenance media containing 10% FCS for 16 hours. Following that, plates were cultured in 4% CCS medium for 5 or 6 days. Cell proliferation was determined by trypsinizing and counting the live cells using trypan blue dye exclusion method every two days. Each cell line was assayed in triplicate and the assay was repeated twice.

Immunohistochemical analysis Histological and IHC analyses were performed as described(10). Briefly, Formalin fixed and paraffin-embedded (PFPE) sections were stained with Hematoxylin and Eosin (HE) or immunohistochemistry. AR (N-20, Santa Cruz) and Ki67 (Vector, VP-RM04) staining were performed as described(7) For fluorescence staining, pretreated sections were first blocked with mouse Ig blocking reagent in the VECTOR M.O.M. Immunodetection Kit (Vector Laboratories) or biotin blocking reagent and then incubated with monoclonal antibody against CK8 (MMS162-P, Covance), SMC (M0851, Dako) at room temperature for 30 min, followed by incubation with Alexa Fluor 594 goat anti-mouse IgG (H+L) (1:1,000; Molecular Probes). Sections were counterstained with DAPI in mounting medium (Vector Laboratories) and analyzed

by fluorescence microscopy.

Karyotyping analysis Cells were allowed to culture until they reached optimum confluency and mitotic stage. The cells were harvested after mitotic arrest with colcemid (0.05µg/mL) for 2 hours. Hypotonization was performed with 0.075M KCl, and a 3:1 mixture of methanol and glacial acetic acid was used for fixation. Slides underwent SKY (Applied Spectral Imaging- ASI, Migdal Ha'Emek, Israel) hybridization, post hybridization, and analyses following standard laboratory procedure. The probe cocktail contained 20 differentially labeled chromosome-specific painting probes and Cot-1 blocking DNA. Image acquisition was performed using a SD300 Spectracube system (ASI) mounted in an Olympus BX60 microscope with a custom-designed optical filter (SKY-1, Chroma Technology, Brattleboro, VT). Ploidy was defined by the chromosome count for each metaphase and was noted by a specific range. Chromosomal gain and/or loss were determined by the average of the observed copy number $\pm$ 25%. Any structural abnormality seen in two or more cells was considered clonal.

Soft agar formation assay Cells were plated at a density of 10,000 cells/plate in 0.3% agar on 6-cm tissue culture dishes coated with 0.6% agar in DMEM growth medium. 20 days after plating, plates were stained with 0.5 ml 0.005% crystal violet. Colonies were counted under light microscope (4x). Only colonies with sizes longer than 0.1mm were included.

In vivo tumor formation study Cells ($1x10^6$) were first mixed with matrigel solution at a ratio of 1:1 and then inoculated subcutaneously on SCID mice (= three months of age).

Tumor formation was observed for 3-8 weeks . Tumor size was determined by caliper measurements, and tumor volume was calculated by a rational ellipse formula (m1 x m1 x m2 x 0.5236, where m1 is the short axis and m2 is the long axis).

Results

Generation of two isogenic prostatic epithelial cell lines from the *Pten* conditional knockout model. To make our investigation of molecular mechanisms underlying PTEN controlled prostate tumorigenesis more amendable, we isolated primary prostatic cells from a hormone naive *Pten*$^{loxp/loxp}$*;PB-Cre4*$^{+}$ mouse. After serial passage and spontaneous immortalization (see Materials and Methods for detail), several clonally derived cell lines were established and from which two lines, named PTEN-P2 and PTEN-P8, were characterized in more detail and are described herein.

Our initial genotyping analysis suggested that PTEN-P2 and PTEN-P8 were heterozygous for *Pten* deletion even though Cre transgene could be easily detected in both lines (Fig.1A, lanes 1 and 3). To rule out possible contamination, two additional rounds of subcloning were performed, which further confirmed the heterozygous status of these two lines (Data not shown). The incomplete deletion of *Pten* loxp alleles led us further investigate the Cre transgene expression, which is under the control of a modified rat probasin (PB) promoter(11). Western blot analysis showed that very low to undetectable Cre protein expression (Fig.1B, lanes 1 and 3) and quantitative reverse transcription-PCR (Q-RT-PCR) analysis confirmed significantly down regulation of the endogenous probasin promoter activity in both cell lines (Fig. 1C). Our recent finding demonstrated that probasin is positively regulated by NKX3.1 and PTEN (12): in the absence of PTEN, NKX3.1 expression as well as its downstream targeting genes, including probasin, are significantly down regulated to undetectable levels in both human and murine prostate cancer tissues (10). Results derived from our current study further

suggest that NKX3.1 and probasin levels are very sensitive to PTEN's dosage effect.

We then infected PTEN-P2 and PTEN-P8 lines with a retrovirus carrying Cre and puromycin drug resistant cassette and the resulting isogenic lines, PTEN-CaP2 and PTEN-CaP8, were generated after two weeks of drug selection. PCR-based genotyping and Western analysis demonstrated that PTEN-CaP2 and PTEN-CaP8 have indeed lost the second $Pten^{loxp}$ allele and are null for PTEN function, as evident by the loss of PTEN protein expression and increased P-AKT levels (Fig, 1A and 1B, lanes 2 and 4). Interestingly, deletion of second allele of *Pten* leads to increased androgen receptor (AR) level, at least in the PTEN-CaP2 cells (comparing AR levels in lanes 1 and 2, Fig. 1B), consistent with our previous finding that PTEN and NKX3.1 serve as negative regulators for AR expression (10).

To determine the cellular origin of these established cell lines, we performed Q-RT-PCR) analysis using primers corresponding to phenotypic markers for the major cell types in the prostates epithelium. As shown in Fig. 1C, all lines co-express both basal (CK14) and luminal cell (CK8/CK18) but not neuroendocrine markers (Fig.1C). Furthermore, PSCA, which represents intermediate stage between basal and luminal cells (Tran et al), is also highly expressed in all four cell lines (Fig.1C)(13). Taken together, these results suggest that the parental PTEN-P2 and P8 lines are most likely originated from intermediate transient amplifying cell population. Interestingly, deletion of the second allele of the *Pten* gene does not lead to significant changes in the expression levels of above marker genes, suggesting that PTEN does not intrinsically control cell differentiation from basal to luminal cells.

PTEN dosage determines tumorigenic potential in vivo. Studies from our group and others demonstrated that PTEN dosage plays a critical role in determine both the onset and progression of prostate cancer (6-8, 14, 15). To examine whether the cell lines we generated can mimic the biological differences between *Pten* heterozygous and homozygous mutants in vivo, we first checked their tumorigenic potentials in vivo on immune incompetent SCID mice. Equal number of cells ($1x10^6$) was injected subcutaneously into the flank of male SCID mice and tumor growth was monitored on a daily basis. Both *Pten* null lines (PTEN-CaP2 and PTEN-CaP8) were tumorigenic with a latency of three weeks. However, no tumor formation could be detected when the same number of *Pten* heterozygous cells (PTEN-P2 and PTEN-P8) were inoculated and followed up to 4 months (Fig. 2A), suggesting that that the dosage effect of PTEN can be recapitulated in these isogenic lines. Histological analysis indicated that all xenograft tumors maintained AR expression and showed luminal epithelial marker CK8 staining but not smooth muscle actin (SMA) staining (Fig. 2B). Similar to our Q-PCR result, no neuroendocrine marker expression could be detected (data not shown), consistent with their epithelial cell origin.

Similar to human prostate cancers, *Pten* null murine prostate cancers do progress to HRPC after castration. To understand whether HRPC development requires additional genetic changes under the hormone deprivation condition, we tested the likelihood of cell lines, which have never been exposed to such a selective pressure, to form tumors on the female mice. Remarkably, both PTEN-CaP2 and PTEN-CaP8 could form tumors on the female SCID mice with similar frequency and latency (Fig. 2A). Histological examination showed no detectable difference in tumors formed by each cell line on either

female or male SCID mice. Ki67 index further confirmed similar proliferation potentials of xenograft tumors generated on both male and female recipient mice (Fig.2C, supplemental figure 1). Thus, PTEN dosage not only dictates the tumorigenic potential but also HRPC development. Our results also suggest that HRPC is an intrinsic property of a cancer cells and its development does not require pre-exposure to hormone deprivation and selection pressure.

Loss of the second allele of *Pten* does not cause global chromosomal alterations. Chromosomal alterations have previously been linked to the progress of prostate cancer(16). To examine whether chromosomal alteration plays the key role in tumorigenesis induced by PTEN loss, we performed karyotyping analyses with a combination of SKY and G-banding tests (Fig. 3) and results are summarized in Table 1. Our study revealed several structural and numerical alterations in each line pairs: PTEN-P2 and PTEN-CaP2 (Supplementary Fig.2) contain near tetraploid chromosome number, with 65-84 chromosomes in PTEN-P2 and 76-80 chromosomes in PTEN-CaP2; PTEN-P8 and PTEN-CaP8 have near 6N chromosomes with 113-125 chromosomes in PTEN-P8 and 115-129 chromosomes in PTEN-CaP8. Importantly, loss of the second allele of *Pten* by Cre retroviral infection did not cause further global structural or numerical changes, at least within the sensitivities of SKY and G-banding analyses offered. Interestingly, all of lines analyzed shared several common chromosomal alterations, including del(7)C-F, -2, +10, +18., which may either support their common origin or reflect basic genetic alterations required for immortalization of epithelial cells (17). Interestingly, loss of the Y chromosome was observed in PTEN-P8 and PTEN-CaP8, which is one of the most frequently cytogenic changes observed in human sporadic prostate tumors(16).

PTEN loss leads to anchorage-independent growth. Since *Pten* loss of heterozygosity (LOH) does not cause additional global chromosomal changes, we searched other mechanisms that might contribute to PTEN controlled tumorigenesis. As a tumor suppressor, PTEN negatively regulates cell cycle progression, cell migration, and cell survival (18). Therefore, PTEN loss is often associated with gain of transformation potential (19). To determine whether *Pten* LOH leads to enhanced transformation potential, we performed soft agar assay. Ten thousand cells were seeded in FCS or CCS growth medium containing 0.3% agar, then with another layer of 0.6% agar on top. After 20 days culture, colonies were photographed and counted. PTEN-CaP2 and PTEN-CaP8 cells formed 5- and 2.5-fold more colonies compared to their parental heterozygous cells, respectively (Fig. 4A). In addition, the general sizes of the colonies formed by *Pten* null cells were larger than those of heterozygous ones (Fig. 4B). Consistent with previous studies, loss of PTEN promotes G1-S transition as PTEN-CaP2 and PTEN-CaP8 cells have decreased amount of G1 cell cycle inhibitor p27 expression, as compared to their isogenic pairs (Fig. 4C). Interestedly, complete loss of PTEN also causes significantly decreased E-cadherin expression (Fig. 4C), a molecule critically important for cell-cell adhesion and tumorigenesis (20).

Loss of PTEN promotes androgen-independent growth in vitro. Since PTEN-CaP2 and PTEN-CaP8 can form tumors in vivo on both male and female SCID mice, we next examined their androgen-independent growth property in the presence of androgen antagonist or in charcoal striped serum environment. We used Casodex, a potent, non-steroidal anti-androgen drug that has been demonstrated to have robust inhibitory effects on the growth of human prostate tumor cell lines, including androgen-dependent cell line

LnCap(21). Consistent with previous literature, Casodex efficiently inhibited LnCap cell growth but it had little effect on the cell lines we generated in this study (Fig.5A), indicating that all four cell lines have acquired androgen-independent growth property.

Consistent with our observation in Casodex treatment, we also observed continuous cell growth in the absence of androgen supplement R1881 in all four cell lines. Although equal number of cells was plated initially, we did observe different cell viability after 5 days in charcoal striped serum (CCS) containing medium. Loss of PTEN allows cells to adapt to the androgen ablated environment more easily: both PTEN-CaP2 and PTEN-CaP8 had a growth advantage as compared to their heterozygote partners (Fig. 5B). During the first 3 days in CCS medium, PTEN-CaP2 has a doubling time about 16hrs while PTEN-P2 has longer doubling time about 26 hrs. Similarly, PTEN-CaP8 has a doubling time of 18.5 hrs while PTEN-P8's doubling time is 26 hrs.

AR is required for PTEN controlled tumorigenesis. Contrary to the AR null androgen-independent PC-3 cells, the *Pten* null prostatic epithelial cell lines we generated are AR positive. Interestedly, PTEN-CaP2 has 1.5 fold in AR protein along with a shorter doubling time compared to PTEN-P2 (Fig.6A top panel). Although PTEN-CaP8 and PTEN-P8 have similar AR protein expression, loss of PTEN increases more AR nuclear translocation compare to PTEN-P8 (Fig.6A low panel). To examine the functional significance of AR in PTEN controlled prostate cancer formation, we used AR RNAi to knock down endogenous AR expression. Primers were generated corresponding to 3 different AR coding regions, after initial analysis, the one showed most significant inhibitory effect was chosen for further functional studies. As shown in Fig. 6B, the

endogenous AR expression in PTEN-CaP2 and PTEN-CaP8 cells were reduced to almost undetectable levels upon RNAi treatment. At the same time, G1 cell cycle inhibitor p21 and p27 levels were significantly increased (Fig. 6B). To measure the biological effects of AR knocking down in *Pten* null cells, we first compared cell growth properties with control RNAi or AR RNAi construct. As shown in Fig. 6C, cell proliferation rates were significantly reduced in both PTEN-CaP2 and -CaP8 cells infected by AR RNAi, suggesting that AR plays an essential role in the cell cycle progression of *Pten* null prostatic epithelial cells. Importantly, AR knocking down significantly impaired the in vivo tumorigenic potentials of *Pten* null cells on female SCID mice (Fig. 6D). Taken together, our results indicate that although PTEN loss cause prostatic epithelial cells to proliferate in the absence of androgen, PTEN controlled prostate tumorigenesis is AR-dependent.

Discussion

One major obstacle to exploring the mechanisms underlying HRPC progression is the shortage of a good system to study, either in vivo or in vitro, that can truly reflect human prostate cancer progression. *Pten* murine prostate cancer model provides a valuable source for studying the mechanism of HRPC. Here we report the characterization of two novel pairs of isogenic prostate cell lines established from the *Pten* null prostate cancer model. Significantly, the novel murine prostate cancer cell lines not only mimic the biological difference between *Pten* heterozygous and homozygous mutants in vivo but also provide the molecular insight into the dosage dependent role of PTEN in tumorigenesis control and androgen responsiveness. Loss of PTEN enables cells to acquire transforming abilities without a significant change in global chromosome structure. Additionally, loss of PTEN promotes androgen independent growth in vivo and in vitro. Through RNAi approach, our study further demonstrates the critical role of AR in PTEN-induced androgen-independent tumorigenesis. Collectively, the novel murine cell lines established from our *Pten* prostate cancer have distinct advantages as a research tool and provide a unique means for exploring both the molecular mechanism underlying HRPC and the development of new targeted therapies.

One of the interesting observations we made was that we didn't directly obtain *Pten* null epithelial cells from the prostate cancer tissue even though this mouse was genotyped as Pten (l/l, Cre+). There are several reasons that may explain this. First, the Cre gene expression is silenced due to significant decreased Probasin expression. Secondly, current primary mouse cell lines derived from genetically engineered mouse prostate cancer models including TRAMP-C1(22), Myc-CaP(9) and our established lines

here, all share the similar transient amplifying epithelial cell marker: PSCA expression. Therefore, in vitro spontaneous immortalization method may preferentially enrich for certain type of prostate cells. Luminal cells with higher AR and probasin expression, which may have total PTEN deletion, may be selected out during this long-term establishment procedure.

HRPC development is a complex process including clonal selection and adaption(3). John Isaacs has postulated that androgen ablation therapy might fail with the eventual development of HRPC due to a subpopulation of androgen-independent tumor cells being present even before therapy was initiated (23). The fact that we can successfully isolate androgen-independent primary cell lines from the primary prostate tumor that has never been exposed to hormonal ablation further supports this hypothesis that acquisition of androgen independence can be uncoupled from hormone deprivation pressure and selection.

Development to HRPC requires cell becoming tumorigenic and androgen independent. Some genetic changes like Myc transgene overexpression in Myc-CaP can trigger cell transformation; however, additional signal/genetic modification are required for adaption to androgen-independence(9). Our study demonstrated that PTEN can functionally control "two" hits: cell transformation and androgen-independence in the course of HRPC tumor development. Furthermore, along with other group's study, we demonstrated the differential dosage dependent role of PTEN on tumorigenesis and androgen responsiveness. In vivo loss-of-function of *Pten* is sufficient for androgen independence in heterozygous animal (24), however, the onset of PIN lesion is 10 months indicating the onset and progression of prostate cancer is highly PTEN dosage dependent

(6). Similar to in vivo's observation, the heterozygous cell lines PTEN-P2 and PTEN-P8 acquired androgen-independent growth capacity, but they were not tumorigenic until the complete loss of PTEN as demonstrated by in vivo tumor formation and in vitro soft agar colony formation assay in PTEN-CaP2 and PTEN-CaP8. Additionally, complete loss of PTEN promotes androgen-independent growth since PTEN-CaP2 and PTEN-CaP8 have androgen-independent growth advantage both in vitro and in vivo. By comparing the two isogenic cell line karyotyping and molecular signaling profiles, we demonstrated loss of PTEN causes decreased p27 and E-cadherin expression, which may contribute to the enhanced gain of transformation ability in PTEN-CaP2 and PTEN-CaP8. Therefore, consistent with recent evidence that loss of PTEN is associated with progression to HRPC(25, 26), our study further underscores the critical role of PTEN in the HRPC development.

Mounting evidence suggest that AR plays an important role in prostate cancer progression(27, 28). Though androgen receptor remains critical for cell-cycle progression in androgen-independent CWR22(29) and LAPC4(30), the specific role of AR in PTEN controlled HRPC progression isn't clearly defined yet. In agreement with previous literature(31, 32), our study suggests that PTEN can regulate AR through multiple mechanisms. We demonstrated that Nkx3.1, a prostate specific tumor suppressor positively regulated by PTEN, can negatively regulate AR expression at the transcriptional level in both the human cell line LnCap and the murine cell line PTEN-CaP2 (10). In this study, there were increased AR transcripts and protein expression following PTEN total deletion in PTEN-CaP2 (Fig.1C, Fig.5B); in PTEN-CaP8, loss of PTEN triggers more nuclear AR translocation in androgen-ablated condition compare to

isogenic line PTEN-P8 (Fig.5A). Significantly, after knocking down endogenous AR expression in PTEN-CaP2 and PTEN-CaP8 cells, RNAi-infected cells displayed a decreased capacity to grow in the androgen-depleted medium and less tumorigenesis potential in vivo, which in part may be due to the increased expression of p21 and p27, G1 cell cycle inhibitors. Therefore, our study confirmed AR is an important cell cycle regulator (33) and further highlight the critical role of AR activation in loss of PTEN induced HPRC development.

Since PTEN-P2 and PTEN-P8 still carry one allele of Pten and were not tumorigenic in vivo, they will serve as an appropriate control to pair with PTEN-CaP2 and PTEN-CaP8 for delineating PTEN regulated signaling pathways in prostate cancer control. Additionally, PTEN-CaP2 and PTEN-CaP8 cells are very easy to maintain in culture and can be readily manipulated by transfection and infection. Their continued growth in androgen-ablated environment also provides a unique avenue for pre-screening drugs efficient for HRPC inhibition. Taken together, these novel prostate cell lines will serve as useful tools for understanding signaling pathways controlled by PTEN and elucidating the molecular mechanisms involved in hormone refractory prostate cancer formation.

ACKNOWLEDGEMENT

We thank Rachel Kim, Sherly Mosessian and colleagues in Wu laboratories for helpful comments and suggestion; JJ is supported by the DOD postdoctoral fellowship Grant W81XWH-04-1-0824. This work is partly supported by funds from DOD PC031130 and NCI UO1 CA84128-06 and RO1 CA107166 (for HW).

References

1. Jemal, A., Murray, T., Samuels, A., Ghafoor, A., Ward, E., and Thun, M. J. Cancer statistics, 2003. CA Cancer J Clin, *53:* 5-26, 2003.
2. Feldman, B. J. and Feldman, D. The development of androgen-independent prostate cancer. Nat Rev Cancer, *1:* 34-45, 2001.
3. So, A., Gleave, M., Hurtado-Col, A., and Nelson, C. Mechanisms of the development of androgen independence in prostate cancer. World J Urol, *23:* 1-9, 2005.
4. Dahia, P. L. PTEN, a unique tumor suppressor gene. Endocr Relat Cancer, *7:* 115-129, 2000.
5. Berger, R., Febbo, P. G., Majumder, P. K., Zhao, J. J., Mukherjee, S., Signoretti, S., Campbell, K. T., Sellers, W. R., Roberts, T. M., Loda, M., Golub, T. R., and Hahn, W. C. Androgen-induced differentiation and tumorigenicity of human prostate epithelial cells. Cancer Res, *64:* 8867-8875, 2004.
6. Trotman, L. C., Niki, M., Dotan, Z. A., Koutcher, J. A., Di Cristofano, A., Xiao, A., Khoo, A. S., Roy-Burman, P., Greenberg, N. M., Van Dyke, T., Cordon-Cardo, C., and Pandolfi, P. P. Pten dose dictates cancer progression in the prostate. PLoS Biol, *1:* E59, 2003.
7. Wang, S., Gao, J., Lei, Q., Rozengurt, N., Pritchard, C., Jiao, J., Thomas, G. V., Li, G., Roy-Burman, P., Nelson, P. S., Liu, X., and Wu, H. Prostate-specific deletion of the murine Pten tumor suppressor gene leads to metastatic prostate cancer. Cancer Cell, *4:* 209-221, 2003.
8. Ma, X., Ziel-van der Made, A. C., Autar, B., van der Korput, H. A., Vermeij, M., van Duijn, P., Cleutjens, K. B., de Krijger, R., Krimpenfort, P., Berns, A., van der Kwast, T. H., and Trapman, J. Targeted biallelic inactivation of Pten in the mouse prostate leads to prostate cancer accompanied by increased epithelial cell proliferation but not by reduced apoptosis. Cancer Res, *65:* 5730-5739, 2005.
9. Watson, P. A., Ellwood-Yen, K., King, J. C., Wongvipat, J., Lebeau, M. M., and Sawyers, C. L. Context-dependent hormone-refractory progression revealed through characterization of a novel murine prostate cancer cell line. Cancer Res, *65:* 11565-11571, 2005.
10. Lei, Q., Jiao, J., Xin, L., Chang, C. J., Wang, S., Gao, J., Gleave, M. E., Witte, O. N., Liu, X., and Wu, H. NKX3.1 stabilizes p53, inhibits AKT activation, and blocks prostate cancer initiation caused by PTEN loss. Cancer Cell, *9:* 367-378, 2006.
11. Wu, X., Wu, J., Huang, J., Powell, W. C., Zhang, J., Matusik, R. J., Sangiorgi, F. O., Maxson, R. E., Sucov, H. M., and Roy-Burman, P. Generation of a prostate

epithelial cell-specific Cre transgenic mouse model for tissue-specific gene ablation. Mech Dev, *101:* 61-69, 2001.
12. Kasper, S. Survey of genetically engineered mouse models for prostate cancer: analyzing the molecular basis of prostate cancer development, progression, and metastasis. J Cell Biochem, *94:* 279-297, 2005.
13. Tran, C. P., Lin, C., Yamashiro, J., and Reiter, R. E. Prostate stem cell antigen is a marker of late intermediate prostate epithelial cells. Mol Cancer Res, *1:* 113-121, 2002.
14. Freeman, D., Lesche, R., Kertesz, N., Wang, S., Li, G., Gao, J., Groszer, M., Martinez-Diaz, H., Rozengurt, N., Thomas, G., Liu, X., and Wu, H. Genetic background controls tumor development in PTEN-deficient mice. Cancer Res, *66:* 6492-6496, 2006.
15. Di Cristofano, A., Pesce, B., Cordon-Cardo, C., and Pandolfi, P. P. Pten is essential for embryonic development and tumour suppression. Nat Genet, *19:* 348-355, 1998.
16. Brothman, A. R. Cytogenetics and molecular genetics of cancer of the prostate. Am J Med Genet, *115:* 150-156, 2002.
17. Zhao, J. J., Gjoerup, O. V., Subramanian, R. R., Cheng, Y., Chen, W., Roberts, T. M., and Hahn, W. C. Human mammary epithelial cell transformation through the activation of phosphatidylinositol 3-kinase. Cancer Cell, *3:* 483-495, 2003.
18. Stiles, B., Groszer, M., Wang, S., Jiao, J., and Wu, H. PTENless means more. Dev Biol, *273:* 175-184, 2004.
19. Boehm, J. S., Hession, M. T., Bulmer, S. E., and Hahn, W. C. Transformation of human and murine fibroblasts without viral oncoproteins. Mol Cell Biol, *25:* 6464-6474, 2005.
20. Jennbacken, K., Gustavsson, H., Welen, K., Vallbo, C., and Damber, J. E. Prostate cancer progression into androgen independency is associated with alterations in cell adhesion and invasivity. Prostate, 2006.
21. Waller, A. S., Sharrard, R. M., Berthon, P., and Maitland, N. J. Androgen receptor localisation and turnover in human prostate epithelium treated with the antiandrogen, casodex. J Mol Endocrinol, *24:* 339-351, 2000.
22. Foster, B. A., Gingrich, J. R., Kwon, E. D., Madias, C., and Greenberg, N. M. Characterization of prostatic epithelial cell lines derived from transgenic adenocarcinoma of the mouse prostate (TRAMP) model. Cancer Res, *57:* 3325-3330, 1997.
23. Isaacs, J. T. The biology of hormone refractory prostate cancer. Why does it develop? Urol Clin North Am, *26:* 263-273, 1999.
24. Gao, H., Ouyang, X., Banach-Petrosky, W. A., Shen, M. M., and Abate-Shen, C. Emergence of androgen independence at early stages of prostate cancer progression in nkx3.1; pten mice. Cancer Res, *66:* 7929-7933, 2006.
25. Mulholland, D. J., Dedhar, S., Wu, H., and Nelson, C. C. PTEN and GSK3beta: key regulators of progression to androgen-independent prostate cancer. Oncogene, *25:* 329-337, 2006.
26. Bertram, J., Peacock, J. W., Fazli, L., Mui, A. L., Chung, S. W., Cox, M. E., Monia, B., Gleave, M. E., and Ong, C. J. Loss of PTEN is associated with progression to androgen independence. Prostate, 2006.

27. Balk, S. P. Androgen receptor as a target in androgen-independent prostate cancer. Urology, *60:* 132-138; discussion 138-139, 2002.
28. Debes, J. D. and Tindall, D. J. Mechanisms of androgen-refractory prostate cancer. N Engl J Med, *351:* 1488-1490, 2004.
29. Yuan, X., Li, T., Wang, H., Zhang, T., Barua, M., Borgesi, R. A., Bubley, G. J., Lu, M. L., and Balk, S. P. Androgen receptor remains critical for cell-cycle progression in androgen-independent CWR22 prostate cancer cells. Am J Pathol, *169:* 682-696, 2006.
30. Chen, C. D., Welsbie, D. S., Tran, C., Baek, S. H., Chen, R., Vessella, R., Rosenfeld, M. G., and Sawyers, C. L. Molecular determinants of resistance to antiandrogen therapy. Nat Med, *10:* 33-39, 2004.
31. Nan, B., Snabboon, T., Unni, E., Yuan, X. J., Whang, Y. E., and Marcelli, M. The PTEN tumor suppressor is a negative modulator of androgen receptor transcriptional activity. J Mol Endocrinol, *31:* 169-183, 2003.
32. Lin, H. K., Hu, Y. C., Lee, D. K., and Chang, C. Regulation of androgen receptor signaling by PTEN (phosphatase and tensin homolog deleted on chromosome 10) tumor suppressor through distinct mechanisms in prostate cancer cells. Mol Endocrinol, *18:* 2409-2423, 2004.
33. Haag, P., Bektic, J., Bartsch, G., Klocker, H., and Eder, I. E. Androgen receptor down regulation by small interference RNA induces cell growth inhibition in androgen sensitive as well as in androgen independent prostate cancer cells. J Steroid Biochem Mol Biol, *96:* 251-258, 2005.

Fig. 1 Characterization of two pairs of novel prostate cell line (PTEN-P2, PTEN-CaP2 and PTEN-P8, PTEN-CaP8) derived from Pten conditional knockout mice with prostate cancer.

A. Genotyping analysis of established cell lines. 1=PTEN-P2, 2=PTEN-CaP2, 3=PTEN-P8, 4=PTEN-CaP8, 5=Lox/Lox, Cre-, 6=Lox/+, Cre+.

B. PTEN-CaP2 and PTEN-CaP8 have AR expression and higher phosphor-Akt level. Western analysis of PTEN, AR, Akt, Cre expression in the established cell lines.

C. Real time PCR analysis of phenotypic marker for prostate cells. CK, cytokeratin; CgA, chromogranin A; Syph, synaptophysin.

Fig.2 PTEN-CaP2 and PTEN-CaP8 are tumorigenic and each has androgen-independent proliferation *in vivo.*

A. PTEN-P2, PTEN-CaP2 and PTEN-P8, PTEN-CaP8 were injected subcutaneously into SCID mice (n=6) and tumor incidence at 60 days was compared.

B. Histology and AR, cytokeratin expression of PTEN-CaP8 tumors. All section are shown at 40x.

C. Ki67 index of xenograft tumors from female and male SCID mice.

Fig. 3 Representative karyotype of the PTEN-CaP8 cell line.

Sequential G-banding (A) and SKY (B) analysis were performed on metaphase preparations derived from PTEN-CaP8 cells. The chromosomal number is variable, but near 6N. One or two markers (M1, M2) as a small fragment of unknown origin.

Fig.4 Soft agar analysis of colony formation for PTEN-P8 and PTEN-CaP8 in FCS medium.

A, Bar graph showing the relative number of colony formation difference.

B. Representative picture showing the colony size formed by PTEN-P8 and PTEN-CaP8.

C. PTEN-CaP2 and PTEN-CaP8 had less p27, and E-cadherin expression compare to their heterozyte line. lower panel right, relatively AR protein expression between the two cell pairs. The density of AR band was normalized by b-Actin as a loading control.

Fig. 5 Loss of PTEN promotes androgen-independent growth *in vitro*.

A. PTEN-P2, PTEN-CaP2 and PTEN-P8, PTEN-CaP8 have resistance to anti-androgen treatment. Cell growth behavior after 3 days Casodex(10uM) treatment.

B. PTEN-CaP2 and PTEN-CaP8 have growth advantage compare to PTEN-P2, PTEN-P8 in CCS medium. Growth curve of the established isogenic cell lines in CCS medium.

Fig. 6 AR is required for PTEN controlled androgen indepependent tumorigenesis.

A. AR expression and localization of established prostate cell lines in CCS medium.

B. Knock down of AR expression cause significant increased p21 and p27 in PTEN-CaP2 and PTEN-CaP8. PTEN-CaP2 and PTEN-CaP8 were retrovirally infected with AR-specific shRNAs (RNAi) or negative control shRNA (Con). 72 hours after infection, lysates were made and analyzed by immunoblot with the indicated antibodies.

C. PTEN-CaP2 and PTEN-CaP8 had significant decrease rate of cell growth in CCS medium upon AR being knockn down. 72 hrs after AR-RNAi or control-RNAi infection,

infected PTEN-CaP2 and PTEN-CaP8 from A were seeded and counted every 2 days after seeding in CCS medium.

D. AR inactivation impairs androgen-independent tumor growth in cells in PTEN-CaP2 and PTEN-CaP8 cells. Infected PTEN-CaP2 and PTEN-CaP8 from A were injected subcutaneously into female SCID mice (n=6) and tumor volume was followed over the indicated time periods.

Supplemental figure 1 Immunohistochemical analyses indicate that *PTEN-CaP2 and PTEN-CaP8* were proliferative in xenograft tumors formed from both female and male SCID mice, as indicated by Ki67-positive immunostaining.

Supplemental figure 2 Representative karyotype of the PTEN-CaP2 cell line.

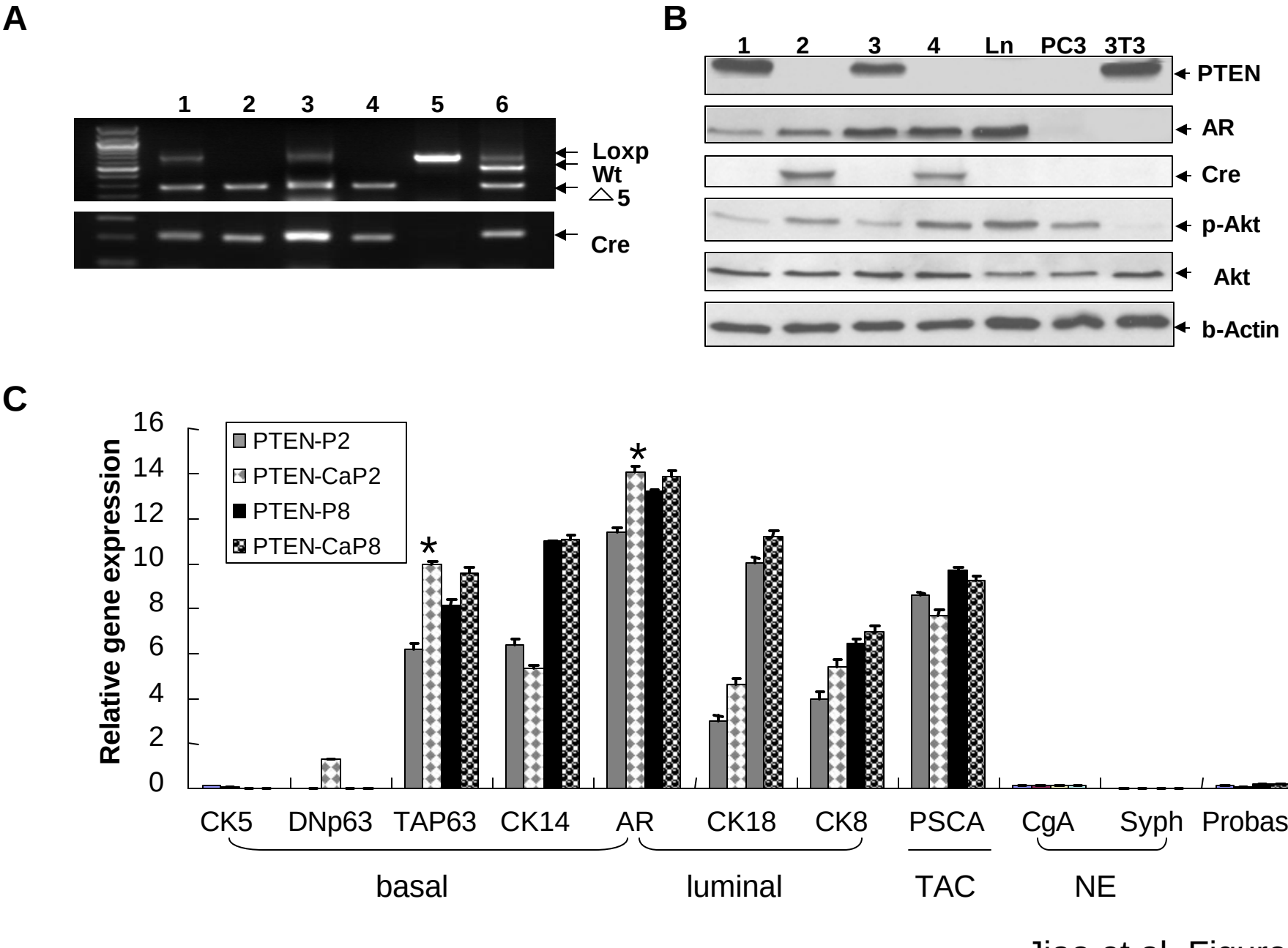

Jiao et al. Figure 1

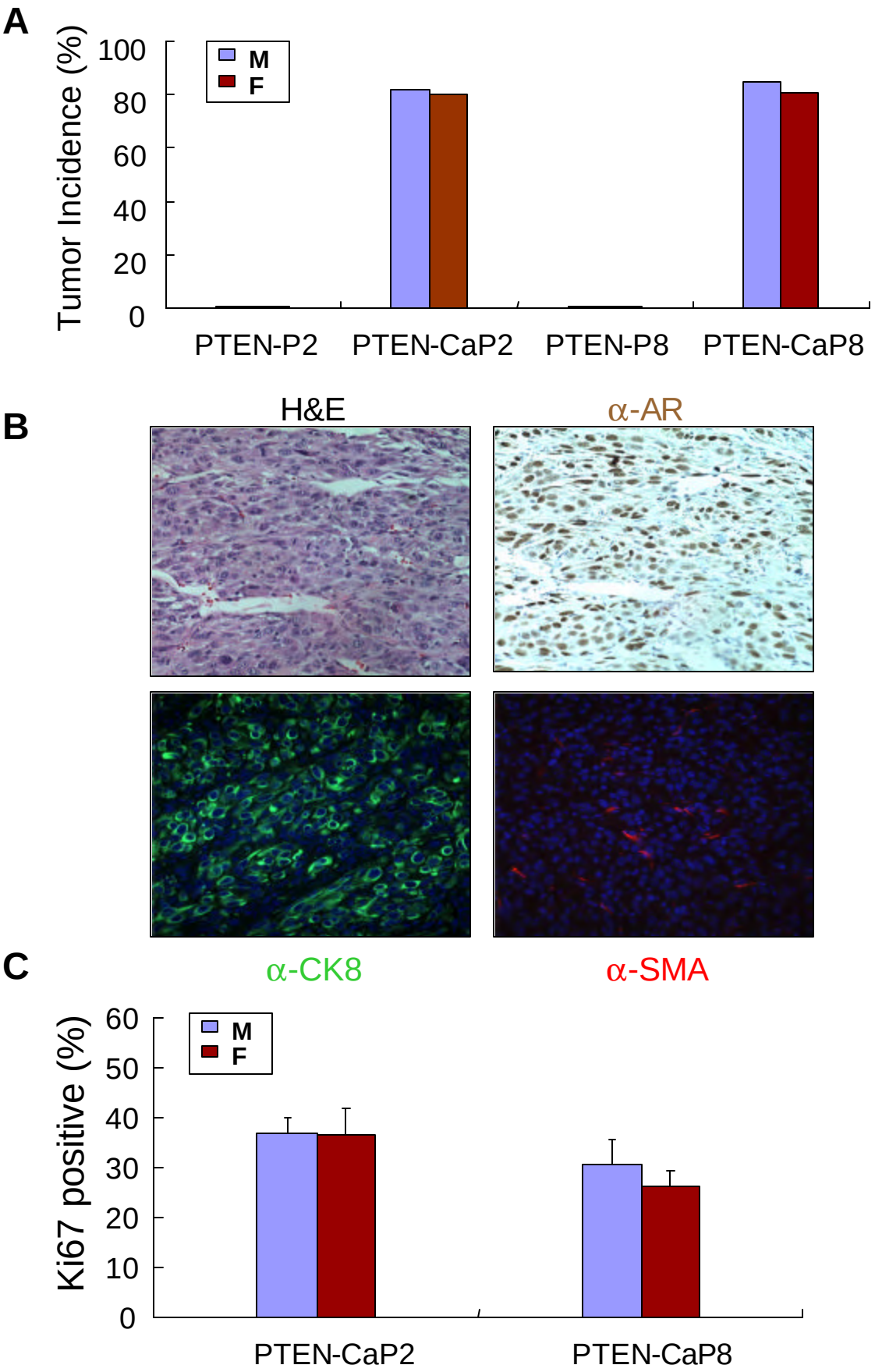

Jiao et al. Figure 2

Table 1 Cytogenic characteristics of established prostate cells

Cell line	Chromosome Count	Numerial Abnormalities	Structure Abnormalities
PTEN-P2	near 4N (65-84)	-2, -4, +10, +13, +15, +18	del(7)C-F
PTEN-CaP2	near 4N (76-80)	-2, +10, +13, +15, +18	del(7)C-F
PTEN-P8	near 6N (113-125)	-1, -2, -4, +10, +17, +18, -Y	der(2)t(2;11), del(7)C-F, del(8)A3-E, del(10)A1-D, del(13)B-D, del(14)C1-E, del(15)B-F
PTEN-CaP8	near 6N (115-129)	-1, -2, -4, +10, +17, +18, -Y	del(5)B-G, del(7)C-F, del(8)A3-E, del(10)A1-D, del(13)B-D, del(14)C1-E, del(15)B-F

A

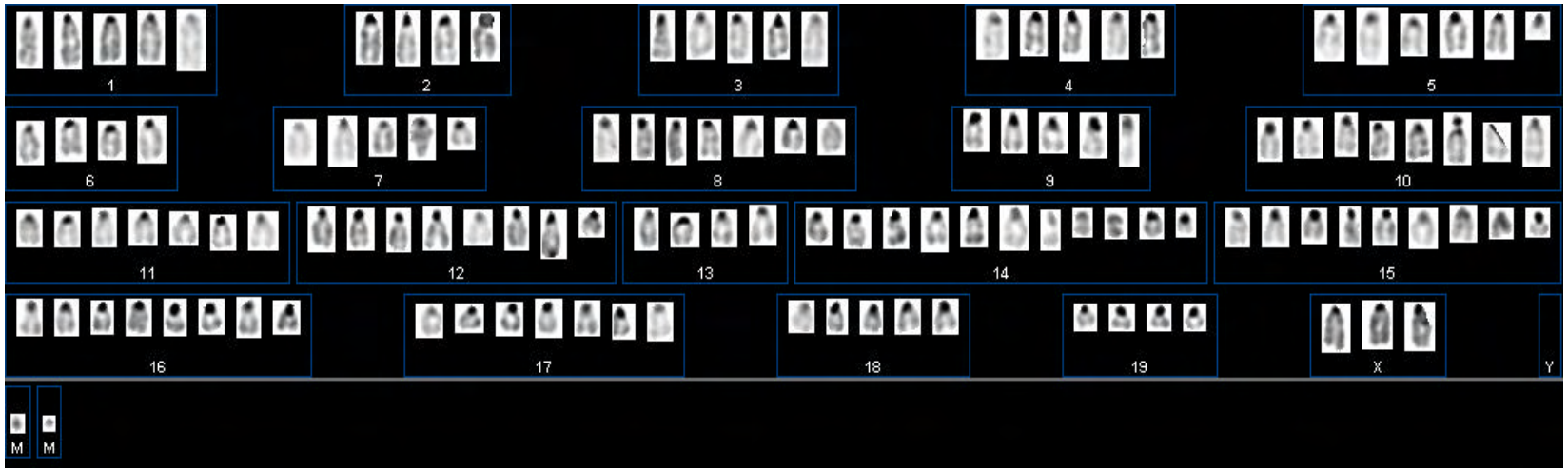

B

Jiao et al. Figure 3

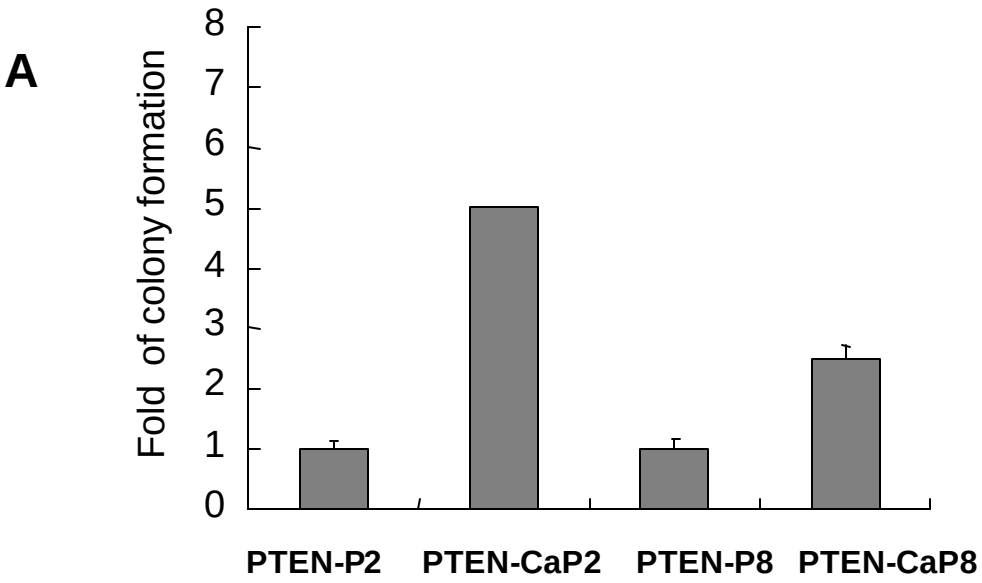

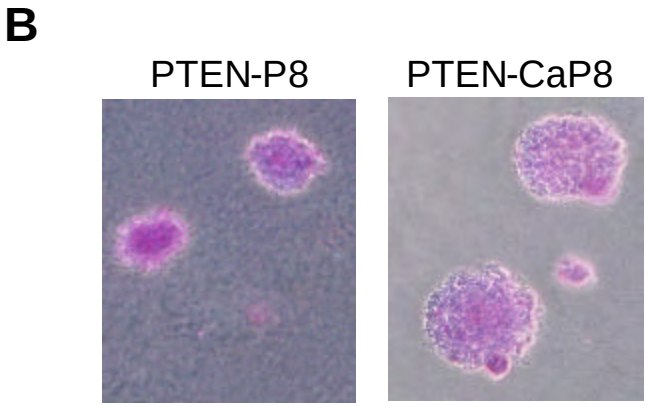

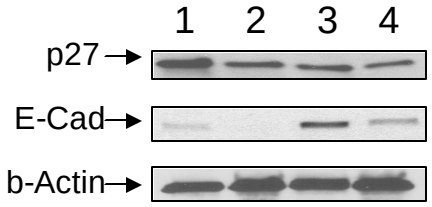

Jiao et al. Figure 4

Jiao et al. Figure 5

A

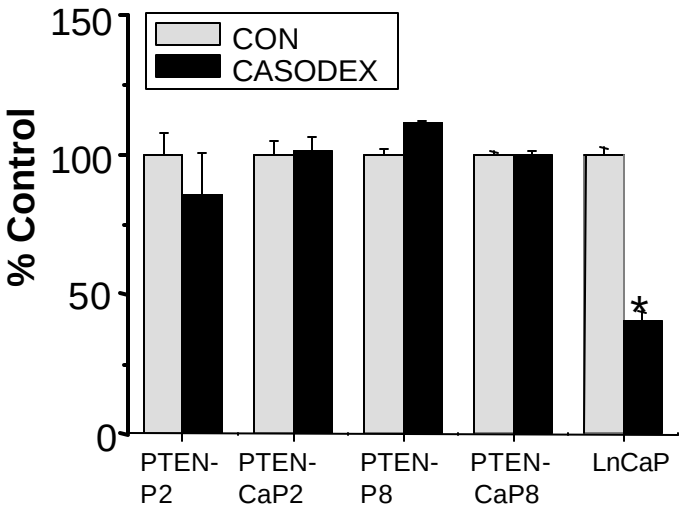

B

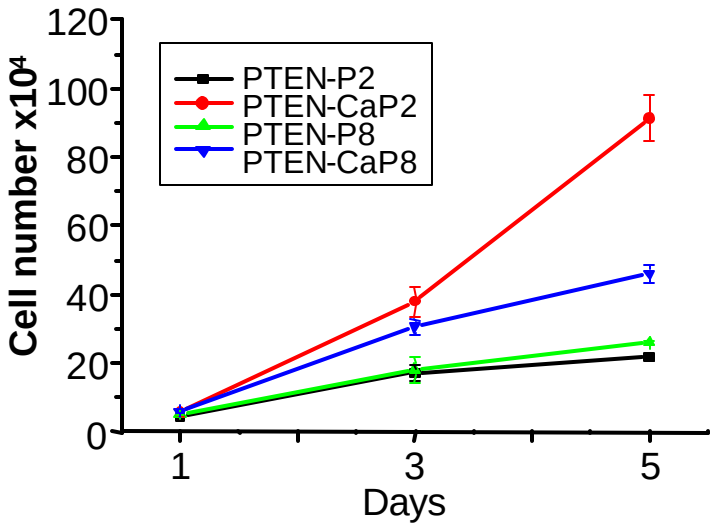

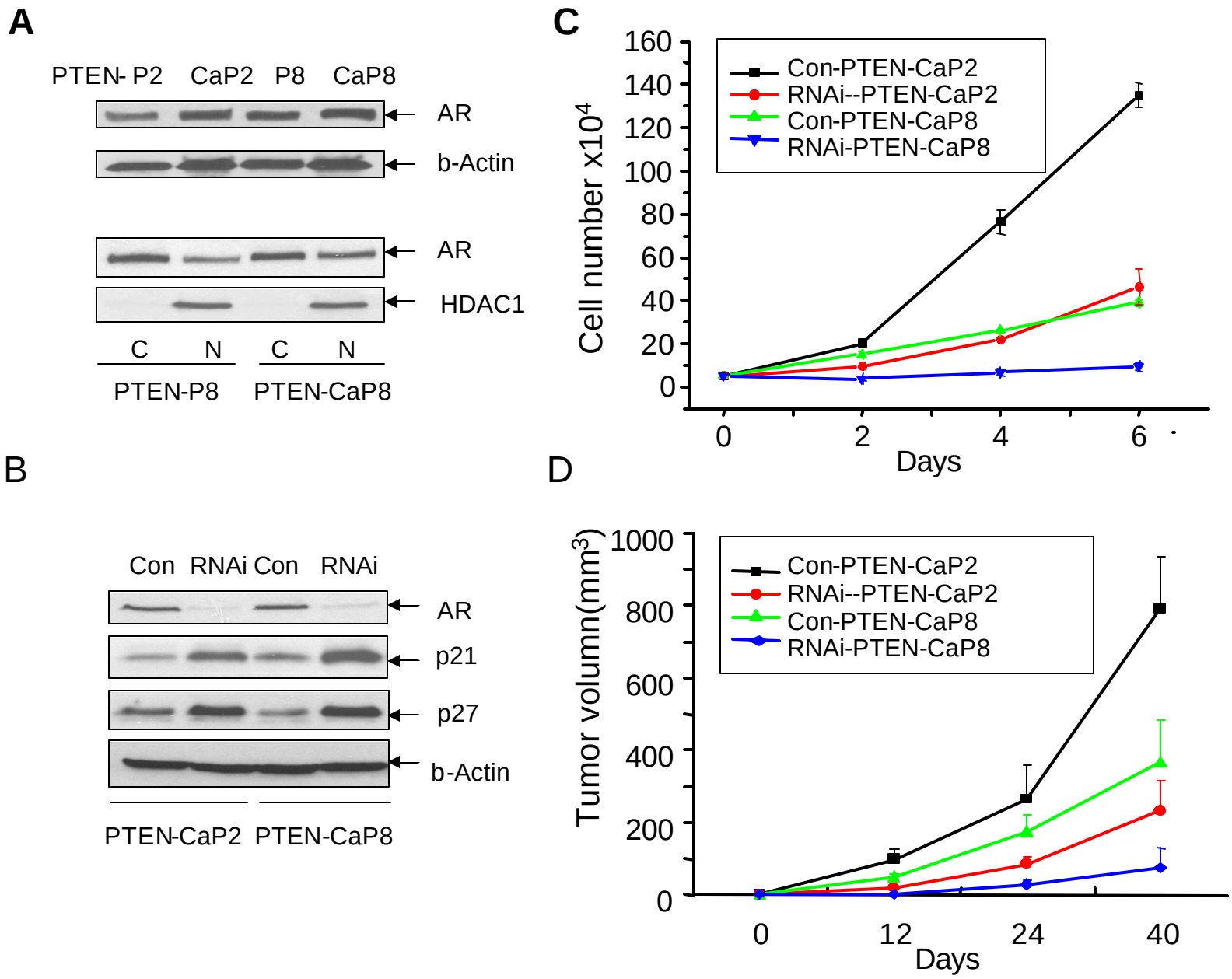

Jiao et al. Figure 6

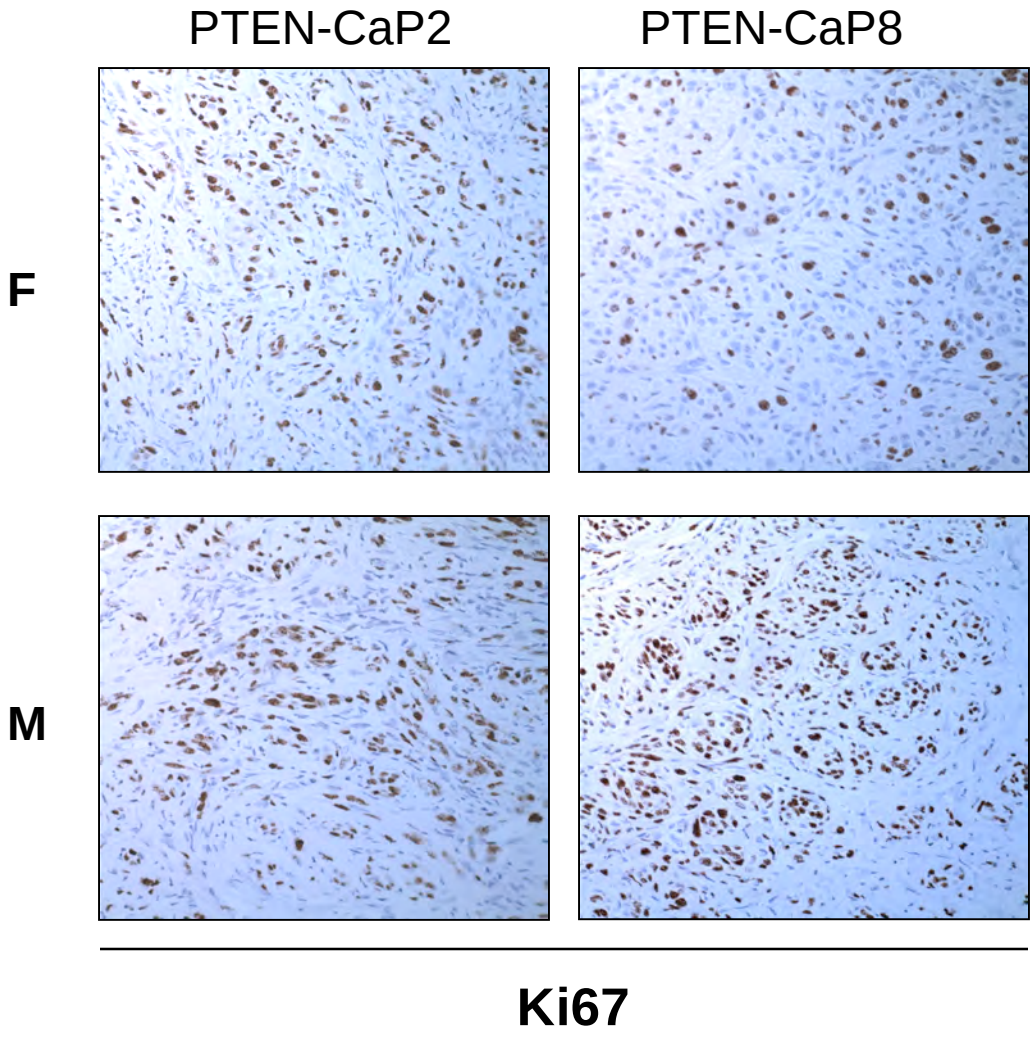

Jiao et al. Supplemental Figure 1

A

B

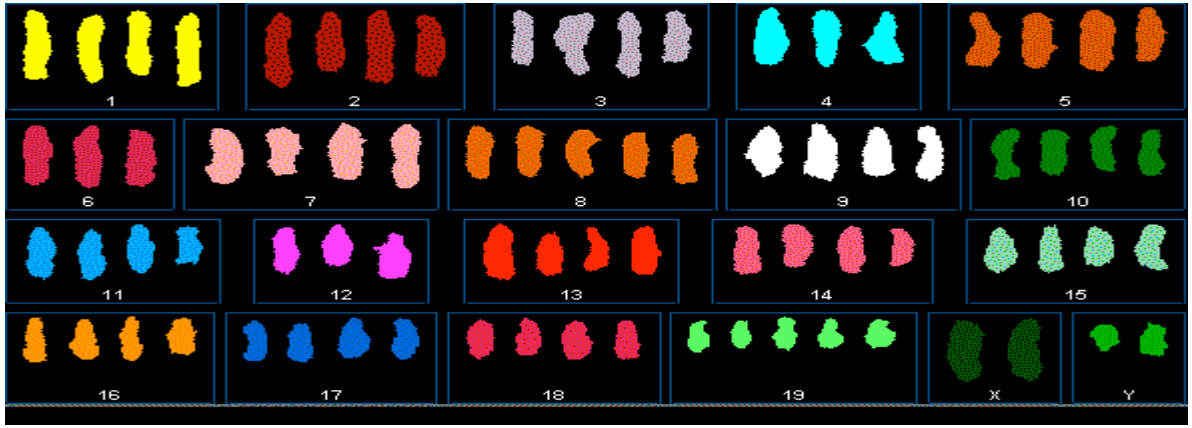

Jiao et al. Supplemental Figure 2